# Structure and Interactive Properties of Highly Fluorinated Phospholipid Bilayers

Thomas J. McIntosh,* Sidney A. Simon,#§ Pierre Vierling,¶ Catherine Santaella,¶ and Veronique Ravily¶
Departments of *Cell Biology, #Neurobiology, and §Anesthesiology, Duke University Medical Center, Durham, North Carolina 27710 USA, and ¶Laboratoire de Chimie Moléculaire, URA 426 au CNRS, Faculté des Sciences, Université de Nice-Sophia Antipolis, 06108 Nice Cédex 2, France

ABSTRACT Because liposomes containing fluoroalkylated phospholipids are being developed for in vivo drug delivery, the structure and interactive properties of several fluoroalkylated glycerophosphocholines (PCs) were investigated by x-ray diffraction/osmotic stress, dipole potential, and hydrophobic ion binding measurements. The lipids included PCs with highly fluorinated tails on both alkyl chains and PCs with one hydrocarbon chain and one fluoroalkylated chain. Electron density profiles showed high electron density peaks in the center of the bilayer corresponding to the fluorine atoms. The height and width of these high density peaks varied systematically, depending on the number of fluorines and their position on the alkyl chains, and on whether the bilayer was in the gel or liquid crystalline phase. Wide-angle diffraction showed that in both gel and liquid crystalline bilayers the distance between adjacent alkyl chains was greater in fluoroalkylated PCs than in analogous hydrocarbon PCs. For interbilayer separations of less than about 8 Å, pressure-distance relations for fluoroalkylated PCs were similar to those previously obtained from PC bilayers with hydrocarbon chains. However, for bilayer separations greater than 8 Å, the total repulsive pressure depended on whether the fluoroalkylated PC was in a gel or liquid-crystalline phase. We argue that these pressure-distance relations contain contributions from both hydration and entropic repulsive pressures. Dipole potentials ranged from −680 mV for PCs with both chains fluoroalkylated to −180 mV for PCs with one chain fluoroalkylated, compared to +415 mV for egg PC. The change in dipole potential as a function of subphase concentration of tetraphenylboron was much larger for egg PC than for fluorinated PC monolayers, indicating that the fluorine atoms modified the binding of this hydrophobic anion. Thus, compared to conventional liposomes, liposomes made from fluoroalkylated PCs have different binding properties, which may be relevant to their use as drug carriers.

## INTRODUCTION

The substitution of fluorine for hydrogen in the hydrophobic chains of phospholipids influences both physicochemical and biological activity. Thus, difluoromethylene-labeled phospholipids have nonideal mixing properties with their hydrocarbon analogs (Sturtevant et al., 1979) and have structural differences (Tristram-Nagle and Dowd, 1994). Compared to conventional hydrocarbon phospholipid liposomes, liposomes formed from phospholipids containing chains with highly fluorinated tails (such as shown in Fig. 1) have 1) modified thermotropic phase behavior (Santaella et al., 1994; Vierling et al., 1995) and dynamics (Santaella and Vierling, 1995), 2) reduced solubility for lipophilic probes (Santaella et al., 1994), 3) reduced membrane permeability (Frézard et al., 1994a,b), and 4) increased stability in biological media (in terms of release of entrapped probes) (Frézard et al., 1994a,b). Several of these highly fluoroalkylated phosphatidylcholines form stable liposomes both above and below the main thermal transition (Santaella et al., 1994). Although no detailed analysis of their structure has been performed, it has been argued that in these bilayers the fluorinated tails are localized in the center of the bilayer, creating a lipophobic fluorocarbon layer surrounded by lipophilic shells formed by the hydrocarbon portions of the chains (Santaella et al., 1993).

Fluorinated phospholipids are of biological interest because the high sensitivity of fluorine-19 NMR enables them to be identified in membranes and because liposomes composed of highly fluoroalkylated phospholipids are currently being investigated as vehicles for in vivo drug delivery (Frézard et al., 1994a,b; Riess, 1994; Vierling et al., 1995; Riess et al., 1996). Necessary requirements for liposomal drug carriers are the ability to encapsulate specific drugs, compatibility with biological tissues, and prolonged stability in the blood vasculature. Liposomes formed from fluorine-modified phosphatidylcholines fulfill, to some extent, these requirements. These liposomes can be efficiently loaded with anticancer drugs (Frézard et al., 1994a) and are biocompatible with mice and cells in culture (Santaella et al., 1991; Vierling et al., 1995; Ravily et al., 1996). Importantly, liposomes made from highly fluorinated PCs have extended in vivo blood circulation times (Santaella et al., 1993; Frézard et al., 1994a,b).

To remain in the blood circulation for extended periods, liposomes must not only have stable bilayer structures, but must be able to avoid ingestion by tissue macrophages that recognize proteins such as opsonins bound to the liposomes

*Received for publication 22 April 1996 and in final form 26 July 1996.*

Address reprint requests to Dr. Thomas J. McIntosh, Department of Cell Biology, Duke University Medical Center, Box 3011, Durham, NC 27710. Tel.: 919-684-8950; Fax: 919-684-3687; E-mail: tom_mcintosh@cellbio.duke.edu.

The present address of Dr. Vierling, Dr. Santaella, and Dr. Ravily is Laboratoire de Chimie Bio-Organique 3, EP 104 au CNRS, Faculté des Sciences, Université de Nice-Sophia Antipolis, 06108 Nice Cédex 2, France.



0006-3495/96/10/1853/16 $2.00

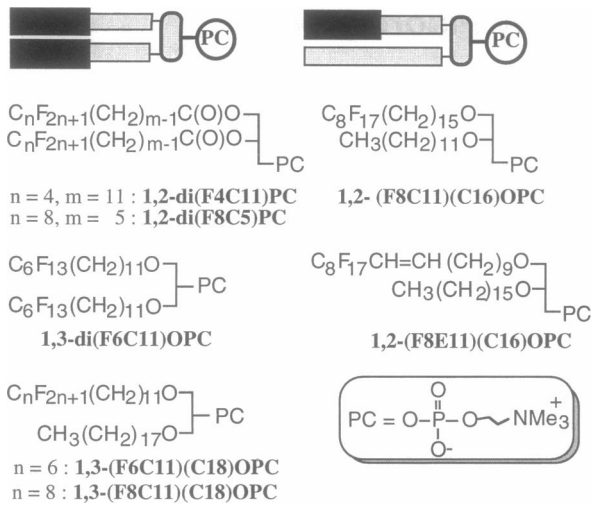


FIGURE 1 Molecular structures of the fluorocarbon/fluorocarbon and mixed-chain fluorocarbon/hydrocarbon glycerophosphocholine molecules used in this study.

(Semple et al., 1996). Conventional liposomes injected into the bloodstream quickly bind serum proteins (Semple et al., 1996), are taken up by macrophages located primarily in the liver or spleen, and therefore cannot be efficiently targeted to other regions of the body. In addition to fluorinated liposomes, liposomes containing phospholipids with covalently attached polyethylene glycol (PEG) have also been shown to have extended blood circulation times (Blume and Cevc, 1990; Klibanov et al., 1990; Allen et al., 1991; Papahadjopoulos et al., 1991). In the case of PEG-liposomes, this increased blood circulation time has been attributed to the steric repulsive barrier around the liposome provided by the covalently attached PEG, which prevents opsonin from binding to the liposome (Lasic et al., 1991; Papahadjopoulos et al., 1991; Woodle et al., 1992). The range and magnitude of this repulsive barrier have been measured for several different PEG-liposomes (Needham et al., 1992; Kuhl et al., 1994; Kenworthy et al., 1995).

The reasons are not known for the increased blood circulation time for vesicles composed of fluorinated lipids, although it has been suggested that fluorinated vesicles have reduced protein adsorption or differences in the nature of proteins adsorbed compared to conventional liposomes (Santaella et al., 1993; Privitera et al., 1995; Vierling et al., 1995). Because fluorinated PC liposomes are uncharged and do not have receptors, protein binding must be mediated by nonspecific interactions such as hydrophobic, hydration, and van der Waals interactions. At least some nonspecific interactions might be affected by the presence of fluoroalkylated chains in the bilayers. For example, fluorocarbons are quite hydrophobic and display a low affinity for hydrocarbons (Mukerjee and Handa, 1981). Fluorines could modify the van der Waals interaction, because liquid perfluorinated alkanes have lower static dielectric constants than normal alkanes (Lifanova et al., 1992). Fluorines in the bilayer interior should also have a large influence on the dipole potential, because dipole potentials measured in monolayers at air-water interfaces have opposite signs for amphiphiles with terminal $-CH_3$ and $-CF_3$ moieties (Adam, 1968; Miller et al., 1987; Vogel and Möbius, 1988; Taylor et al., 1990). The magnitude of the dipole potential has been related to the magnitude of the repulsive hydration pressure (Simon and McIntosh, 1989; Simon et al., 1992) and to the binding of hydrophobic ions to the bilayer surface (Cafiso, 1995). However, because the dipole potential depends on contributions from all oriented dipoles in the bilayer, including those of the lipid and solvent molecules (Zheng and Vanderkooi, 1992; Chiu et al., 1995; Eβmann et al., 1995), it is difficult to predict the dipole potential of fluoroalkylated phosphatidylcholines with the fluorines distributed on one or more acyl chains. Comparisons of dipole potential data with measurements of pressure-distance relations and hydrophobic ion binding could provide useful information on the interfacial effects of dipoles located deep in the core region of the bilayer. In addition, fluorines could also affect the repulsive undulation pressure by altering the flexibility of the bilayer by virtue of the presence of the $-CF_3$ and $-CF_2$ moieties that occupy a larger volume than the corresponding hydrocarbon moieties.

In this paper we employ several methods to obtain information on the structure and interactive properties of liposomes made from various highly fluorinated phospholipids (Fig. 1). X-ray diffraction analysis of osmotically stressed multilamellar systems is used to determine the structure and pressure-distance relations for bilayers composed of these fluoroalkylated phospholipids. Dipole potentials and binding of hydrophobic ions to monolayers of these lipids are measured and correlated with the observed interbilayer repulsive pressures.

## MATERIALS AND METHODS

### Materials

Bilayers were studied that contained the following fluoroalkylated phosphatidylcholines: 1,2-di(F4C11)PC; 1,2-di(F8C5)PC; 1,3-(F8C11)(C18)-OPC; 1,3-(F6C11)(C18)OPC; 1,2-(F8E11)(C16)OPC; 1,3-di(F6C11)OPC; and 1,2-(F8C11)(C16)OPC. As shown in Fig. 1, these double-chain phospholipids differ in the number of fluorocarbon chains, in the length of the fluorinated tails and hydrocarbon spacers, in the chemical linkages (ester or ether), and in the positions (1,2- or 1,3-) of the chains on the glycerol backbone. The fluorocarbon (di-*O*-acyl) phosphatidylcholines and di-*O*-alkylglycerophosphocholines were synthesized by procedures described in detail by Santaella et al. (1991) and Ravily et al. (1996), respectively. Lipid purity (>99%) was periodically checked by thin-layer chromatography and $^1H$-, $^{13}C$-, and $^{31}P$-NMR. All of these phospholipids are rac-derivatives. Compound 1,2-(F8E11)(C16)OPC consists of a mixture of *cis* and, mainly, *trans* isomer (*cis*/*trans* ≤ 10/90; Ravily et al., 1996). The main phase transition temperatures of these lipids measured by differential scanning calorimetry (DSC) have been found to be 18.6°C for 1,2-di(F4C11)PC; 69.3°C for 1,2-di(F8C5)PC (Santaella et al., 1994); 46.4°C for 1,3-(F8C11)(C18)OPC; 39°C for 1,3-(F6C11)(C18)OPC; 5.1°C for 1,2-(F8E11)(C16)OPC; 52°C for 1,3-di(F6C11)OPC; and 44°C for 1,2-(F8C11)(C16)OPC (Vierling et al., 1995; Ravily et al. 1996).

Sodium tetraphenylboron was obtained from Aldrich Chemical Company (Milwaukee, WI).

## X-ray diffraction

X-ray diffraction analysis was performed on both unoriented suspensions of multiwalled vesicles and oriented multilayers subjected to known osmotic pressures (LeNeveu et al., 1977; Parsegian et al., 1979; McIntosh and Simon, 1986; McIntosh et al., 1987). Osmotic stress was applied to the liposomes by incubating them in aqueous solutions of dextran or PEG. Because these polymers are too large to enter the lipid lattice, they compete for water with the lipid multilayers, thereby applying an osmotic pressure ($P$) (LeNeveu et al., 1977; Parsegian et al., 1979). Pressure was applied to oriented multibilayers by incubating them in constant relative humidity atmospheres maintained with various saturated salt solutions (O'Brien, 1948). In this case, the applied pressure is given by

$$P = -(RT/V_w) \cdot \ln(p/p_o), \quad (1)$$

where $R$ is the molar gas constant, $T$ is the temperature in degrees Kelvin, $p/p_o$ is the ratio of the vapor pressure of the saturated salt solution to the vapor pressure of pure water, and $V_w$ is the partial molar volume of water (Parsegian et al., 1979).

Unoriented suspensions were prepared by adding excess (more than 90% by weight) buffer (100 mM NaCl, 20 mM HEPES, pH 7) or polymer solution and incubating with extensive vortexing above the lipid's phase transition temperature. To facilitate equilibration of the salt across the multilayers, several freeze-thaw cycles were used. Suspensions were pelleted with a bench centrifuge, sealed in quartz glass x-ray capillary tubes, and mounted in a point collimation x-ray camera. Oriented multilayers were formed by drying a small drop of lipid/chloroform solution onto a curved glass substrate. The multilayers on the glass substrate were mounted in a controlled humidity chamber on a single-mirror (line-focused) x-ray camera such that the x-ray beam was oriented at a grazing angle relative to the multilayers (McIntosh et al., 1987, 1989b). The humidity chamber, which contained a cup of the saturated salt solution, consisted of a hollow-walled copper cannister with two Mylar windows for passage of the x-ray beam. To speed equilibration, a gentle stream of nitrogen was passed through a flask of the saturated salt solution and then through the chamber.

For both oriented and unoriented specimens, x-ray diffraction patterns were recorded on Kodak DEF x-ray film. The films were processed by standard techniques and densitometered with a Joyce-Loebl microdensitometer as described previously (McIntosh and Simon, 1986; McIntosh et al., 1987, 1989b). After background subtraction, integrated intensities, $I(h)$, were obtained for each order $h$ by measuring the area under each diffraction peak. For unoriented patterns, the structure amplitude $F(h)$ was set equal to $\{h^2 I(h)\}^{1/2}$ (Blaurock and Worthington, 1966; Herbette et al., 1977). For the oriented line-focused patterns the intensities were corrected by a single factor of $h$ due to the cylindrical curvature of the multilayers (Blaurock and Worthington, 1966; Herbette et al., 1977), so that $F(h) = \{hI(h)\}^{1/2}$.

Information on the structure of the bilayers was obtained by a Fourier analysis of the x-ray data. Electron density profiles, $\rho(x)$, on a relative electron density scale were calculated from

$$\rho(x) = (2/d)\Sigma \exp\{i\phi(h)\} \cdot F(h) \cdot \cos(2\pi xh/d), \quad (2)$$

where $x$ is the distance from the center of the bilayer, $d$ is the lamellar repeat period, $\phi(h)$ is the phase angle for order $h$, and the sum is over $h$. Phase angles were determined by the use of the sampling theorem (Shannon, 1949), as described in detail previously (McIntosh and Simon, 1986; McIntosh and Holloway, 1987; McIntosh et al., 1989a).

As described in the Results, the electron density profiles were used to estimate the distance between bilayers ($d_f$) for each value of applied pressure ($P$). In the presence of an applied osmotic pressure, $d_f$ is determined by the balance of the the interbilayer repulsive pressure ($P_r$) with the sum of $P$ plus the attractive van der Waals pressure ($P_v$), so that $P_r = P_v + P$. For applied pressures such that $p \gg P_v$, $P_r \approx P$ so that plots of log $P$ versus $d_f$ represent the distance dependence of the total repulsive pressure between bilayers (LeNeveu et al., 1977).

## Dipole potential

Dipole potentials ($V$) were measured using monolayers as described previously (MacDonald and Simon, 1987). Monolayers were formed by spreading 10 to 20 μl of a 10 mg/ml lipid in chloroform solution onto a subphase of 0.1 or 1 M NaCl, 1 mM HEPES (pH 7.0) in a trough with a surface area of about 20 $cm^2$. Additional lipid did not produce any change in the dipole potential, indicating that the surface was completely covered and in equilibrium with the visible lenses of lipid. Under these conditions the packing of the lipid molecules in the monolayer is approximately the same as it is in a bilayer (MacDonald and Simon, 1987). The dipole potential was measured at room temperature between a Ag/AgCl electrode in a 4 M KCl reference solution containing silver chloride, connected to an agar bridge in the subphase, and a $^{241}Am$ electrode in air, using a Keithley electrometer (model 602; Keithley Instruments Co., Cleveland, OH). The subphase was stirred with a small Teflon magnetic flea. The reported values of $V$ represent the difference in the potential of the subphase surface in the presence and absence of the lipid monolayer.

## Binding of hydrophobic ions

Small aliquots of stock solutions of sodium tetraphenylboron ($TPB^-$) in 1 M NaCl, 1 mM HEPES at pH 7 were injected into the stirred subphase under the monolayer, and the changes in the dipole potential were recorded on a chart recorder. The steady-state changes in dipole potential ($\Delta V$) are reported in this paper.

# RESULTS

## X-ray diffraction

Dispersions of the fluorinated lipids gave wide-angle x-ray diffraction patterns that contained one to three sharp or broad reflections (Table 1). A single broad reflection is characteristic of lipid bilayers in the melted liquid-crystalline phase, whereas sharp wide-angle reflections (or a mixture of sharp and broad reflections) are typically recorded for gel phase bilayers below their melting (phase transition) temperature (Tardieu et al., 1973). Our assignments of gel or liquid-crystalline phases based on the wide-angle patterns (Table 1) are consistent with the phase transition temperatures of these lipids given in Materials and Methods. An interesting feature of the fluorinated lipids is that, in either the gel or liquid-crystalline phases, the wide-angle reflections were at larger spacings than the corresponding reflections for typical phosphatidylcholine bilayers with hydrocarbon chains (Table 1). It should also be noted that the strong wide-angle reflection of 4.95 Å from 1,2-di(F8C5)PC (Table 1) was very similar in spacing to the single wide-angle reflection at 4.97 Å observed from compressed monolayers of $CF_3$-$(CF_2)_9$-$(CH_2)_2$-OCO-$CH_2$-$CH(NH_3^+)CO_2^-$ (Wolf et al., 1988).

For all oriented and unoriented fluoroalkylated lipid specimens, the low-angle x-ray diffraction patterns consisted of a series of sharp reflections that indexed as orders of a lamellar repeat period. Such lamellar patterns are characteristic of multiple layers of lipid bilayers. The repeat periods at 23°C in excess buffer were 58.5 Å for 1,2-di(F8C5)PC, 59.4 Å for 1,3-(F6C11)OPC, 69.3 Å for 1,2-(F8C11)(C16)OPC, 72.6 Å for 1,2-(F8E11)(C16)OPC, 64.8 Å for 1,3-(F8C11)(C18)OPC, and 61.9 Å for 1,3-

**TABLE 1 X-ray diffraction and dipole potential data**

| Lipid | Temperature (°C) | Bilayer phase | Wide-angle spacings (Å) | $d_{pp}$ (Å) | $d_{fe}$ (Å) | Dipole potential (mV) | $P_o$ ($\times 10^{-8}$ dyn/cm$^2$) |
|---|---|---|---|---|---|---|---|
| 1,2-di(F8C5)PC | 23 | Gel | 4.95 (s) | 37.7 | 10.8 | −680 | 4.7 |
| 1,2-di(F4C11)PC | 12 | Gel | 5.3 (s), 4.6 (s), 4.4 (b) | 35.1 | 14.7 | — | — |
| 1,2-di(F4C11)PC | 23 | l.-c. | 4.8 (b) | — | — | −576 | 5.6 |
| 1,3-di(F6C11)OPC | 23 | Gel | 4.89 (s), 4.67 (b) | 39.5 | 9.9 | −495 | 18.2 |
| 1,2-(F8C11)(C16)OPC | 23 | Gel | 4.56 (s) | 46.5 | 12.8 | −445 | 31.6 |
| 1,2-(F8E11)(C16)OPC | 23 | l.-c. | 4.8 (b) | 45.4 | 17.2 | −485 | 20.4 |
| 1,3-(F8C11)(C18)OPC | 23 | Gel | 4.48 (vs) | 45.4 | 8.8 | −220 | — |
| 1,3-(F6C11)(C18)OPC | 23 | Gel | 4.48 (vs) | 42.7 | 9.2 | −184 | 11.7 |
| EPC* | 20 | l.-c. | 4.6 (b) | 37.8 | 15.4 | +415 | 4.0 |
| 1,2-di(C16)PC* | 20 | Gel | 4.2 (s), 4.0 (b) | 41.9 | 11.7 | +575 | 47.0 |
| 1,2-di(C16)PC* | 10 | Subgel | 4.4 (s), 3.9 (b) | 41.0 | 8.4 | — | 11.1 |

l.-c., liquid crystalline phase; vs, very sharp; s, sharp; b, broad.
*Diffraction data are from McIntosh and Simon (1986, 1993); dipole potential data are from Simon and McIntosh (1989).

(F6C11)(C18)OPC. At 12°C 1,2-di(F4C11)PC had a repeat period of 59.8 Å in excess buffer. These repeat periods in excess buffer are shown on the $x$ axis in Fig. 2.

For each type of fluoroalkylated phosphatidylcholine the lamellar period decreased with increasing applied osmotic pressure. Plots of the logarithm of applied pressure (log $P$) versus lamellar repeat period ($d$) are shown in Fig. 2 for the seven fluorinated lipids. For each lipid, $d$ decreased with increasing applied pressure.

For each specimen the lamellar repeat period is equal to the sum of the thickness of the lipid bilayer ($d_b$) and the fluid space between adjacent bilayers ($d_f$). To obtain information on the structure of the bilayer and the relative sizes of $d_b$ and $d_f$, we performed a Fourier analysis of the diffraction data for each lipid system. Detailed results of this analysis are shown in Figs. 3–7 for four selected lipids. Fig. 3, *A–D*, shows the observed structure amplitudes plotted versus reciprocal space coordinate for gel phase 1,2-di(F4C11)PC, gel phase 1,3-(F8C11)(C18)OPC, gel phase 1,3-(F6C11)(C18)OPC, and liquid-crystalline phase 1,2-(F8E11)(C16)OPC, respectively. The diffraction data extended to larger values of reciprocal space (higher resolution) for the gel phase bilayers. In each plot the solid line corresponds to the continuous transform calculated using the sampling theorem (Shannon, 1949), by procedures detailed in McIntosh and Simon (1986) for one data set (open circles) corresponding to one particular repeat period. Phase angles were chosen so that the continuous transform went through the structure amplitudes for the other data sets (McIntosh and Holloway, 1987).

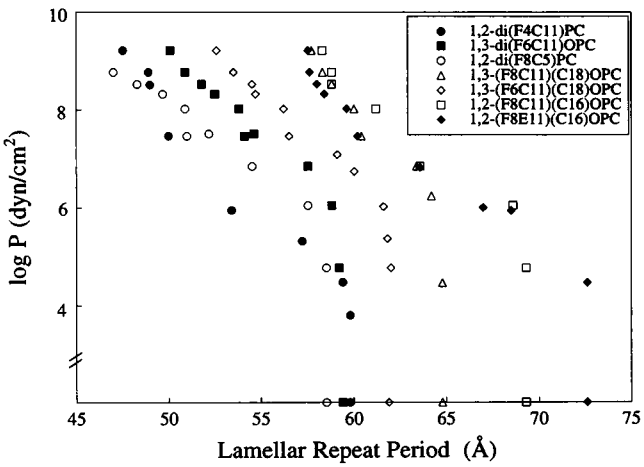


FIGURE 2 Plot of the logarithm of applied pressure (log $P$) versus the lamellar repeat period ($d$) for 1,2-di(F4C11)PC, 1,3-di(F6C11)OPC, 1,2-di(F8C5)PC, 1,3-(F8C11)(C18)OPC, 1,3-(F6C11)(C18)OPC, and 1,2-(F8C11)(C16)OPC in the gel phase, and 1,2-(F8E11)(C16)OPC in the liquid-crystalline phase. The data for 1,2-di(F4C11)PC were recorded at 12°C, and all of the other data were recorded at 23°C. The repeat periods recorded in excess buffer (in the absence of applied pressure) are given on the $x$ axis.

Fig. 4, *A–D*, shows electron density profiles for gel phase 1,2-di(F4C11)PC, gel phase 1,3-(F8C11)(C18)OPC, gel phase 1,3-(F6C11)(C18)OPC, and liquid-crystalline phase 1,2-(F8E11)(C16)OPC, respectively. The profiles in Fig. 4 *A* are at a resolution ($d/2h_{max}$) of about 3 Å, the profiles in Fig. 4, *B* and *C*, are at a resolution of about 5 Å, and the profiles in Fig. 4 *D* are at a resolution of about 7 Å. For each lipid two profiles are shown, corresponding to different applied pressures. In each profile the center of the bilayer is at the origin, the high electron density peaks centered near ±20 Å correspond to the lipid headgroup, and the medium-density regions at the outer edges of each profile correspond to the fluid spaces between adjacent bilayers. The very large electron densities in the center of the bilayer are due to the fluorines in the lipid chains. In the gel phase bilayers (Fig. 4, *A–C*) there was a dip in the geometric center of the profile, probably corresponding to the preferential localization of the terminal $CF_3$ or $CH_3$ groups in the center of the bilayer. It has been shown that $CH_3$ groups have larger volumes (Nagle and Wilkinson, 1978) and smaller electron densities (Lesslauer et al., 1972; Franks, 1976; McIntosh and Simon, 1986) than $CH_2$ groups, and terminal methyl dips are typically seen in the center of hydrogenated phosphatidylcholine bilayers in the gel phase (Fig. 5 and Lesslauer et al., 1972; Torbet and Wilkins, 1976; McIntosh and Simon, 1986). Because the volumes of a $CF_3$ group and a

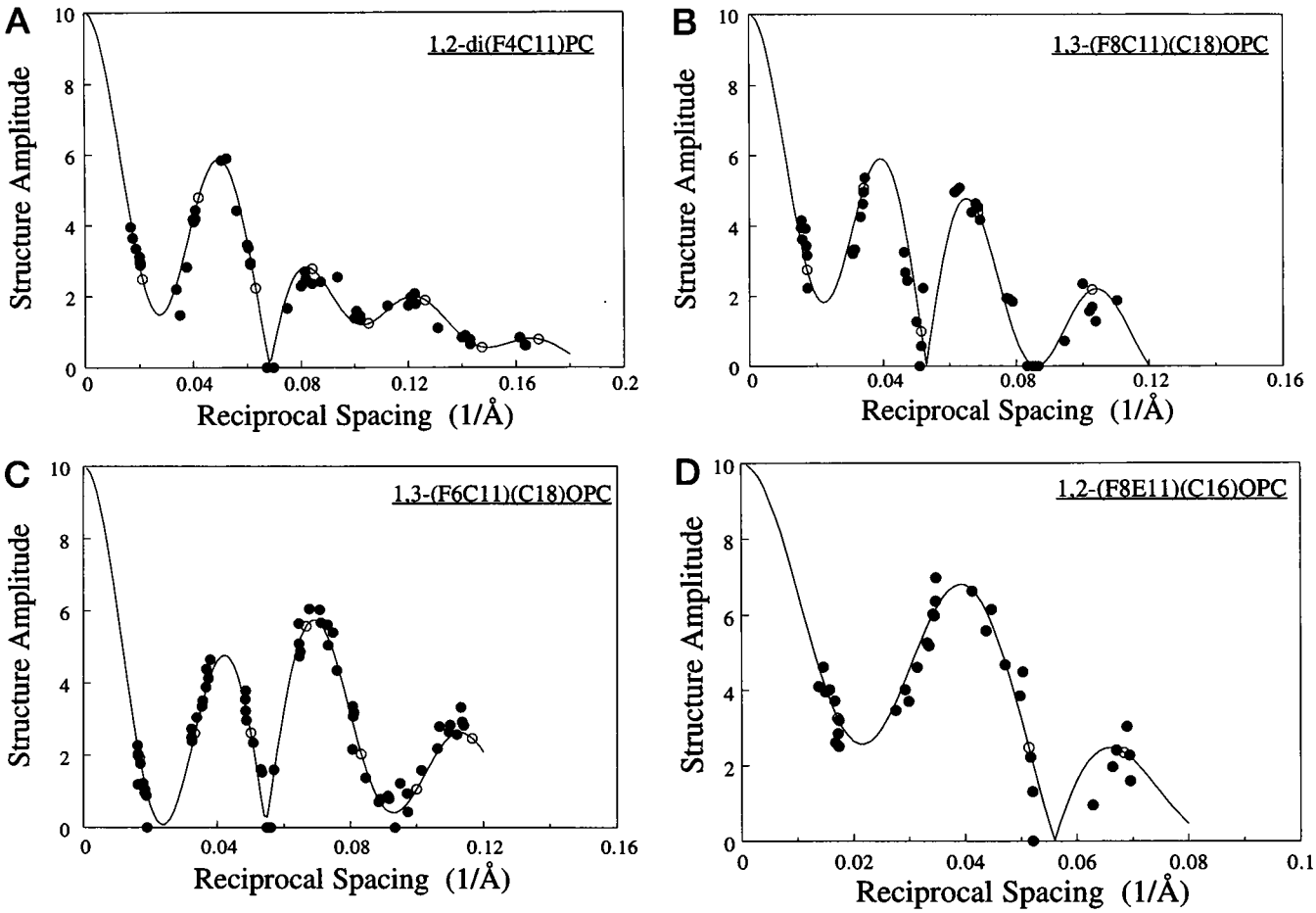


FIGURE 3 Plots of observed structure amplitudes (○, ●) versus reciprocal space coordinate for (*A*) 1,2-di(F4C11)PC, (*B*) 1,3-(F8C11)(C18)OPC, (*C*) 1,3-(F6C11)(C18)OPC, and (*D*) 1,2-(F8E11)(C16)OPC. The solid lines are continuous Fourier transforms calculated with the sampling theorem for one particular data set for each lipid (denoted by *open circles*).

$CF_2$ group are about 92 Å$^3$ and 38 Å$^3$, respectively (Tiddy, 1985), which corresponds to electron densities of 0.29 *e*/Å$^3$ and 0.47 *e*/Å$^3$, respectively, the localization of $CF_3$ groups in the center of the bilayer containing $CF_2$ groups would cause the troughs observed in the center of the profiles in Fig. 4, *A–C*. The profiles of the liquid-crystalline phase 1,2-(F8E11)(C16)OPC (Fig. 4 *D*) did not exhibit an electron density dip in the middle of the profile. This is probably due to both the lower resolution of the profile and the increased disorder in the alkyl chain region, so that the terminal $CF_3$ and $CH_3$ groups were not as well localized.

For each of the profiles in Fig. 4, *A–D*, the bilayer portion of the profile remained nearly constant with increasing applied pressure. In particular, the shape of the profile remained nearly the same, and the distance between headgroup peaks ($d_{pp}$) across the bilayer remained nearly constant as a function of osmotic pressure. When the electron density profiles were calculated at approximately the same resolution ($d/2h_{max} \approx 5$ to 7 Å), the values of $d_{pp}$ (mean ± one standard deviation) were 37.7 ± 0.3 Å ($n = 8$) for 1,2-di(F8C5)PC; 35.1 ± 0.8 Å ($n = 5$ experiments) for 1,2-di(F4C11)PC; 39.5 ± 0.2 Å ($n = 3$) for 1,3-di(F6C11)OPC; 46.5 ± 0.4 Å ($n = 4$) for 1,2-(F8C11)(C16)OPC; 45.4 ± 0.8 Å ($n = 6$) for 1,2-(F8E11)(C16)OPC; 45.4 ± 1.1 Å ($n = 5$) for 1,3-(F8C11)(C18)OPC; and 42.7 ± 0.6 Å ($n = 10$) for 1,3-(F6C11)(C18)OPC (Table 1). These values can be compared to the value of $d_{pp} = 41.9$ Å for the hydrocarbon gel (L$\beta'$) phase lipid, 1,2-di(C16)PC (DPPC) (McIntosh and Simon, 1986). For each lipid, the major difference between the profiles obtained at different osmotic pressures was in the width of the fluid space between bilayers. With increasing osmotic pressure the distance between bilayers decreased as water was removed from the fluid space between bilayers (Fig. 4).

Fig. 5 compares the electron density profile of gel phase 1,2-di(F4C11)PC with that of 1,2-di(C16)PC (DPPC). The profiles were put on the same arbitrary electron density scale by assuming that the electron densities of the PC headgroups were the same in the two bilayers and were calculated at the same resolution ($d/2h_{max} \approx 3$ Å). There were two major differences between these profiles. First, the bilayer width was significantly smaller for 1,2-di(F4C11)PC, even though this fluorinated lipid has only one less carbon per chain than DPPC. Second, the electron

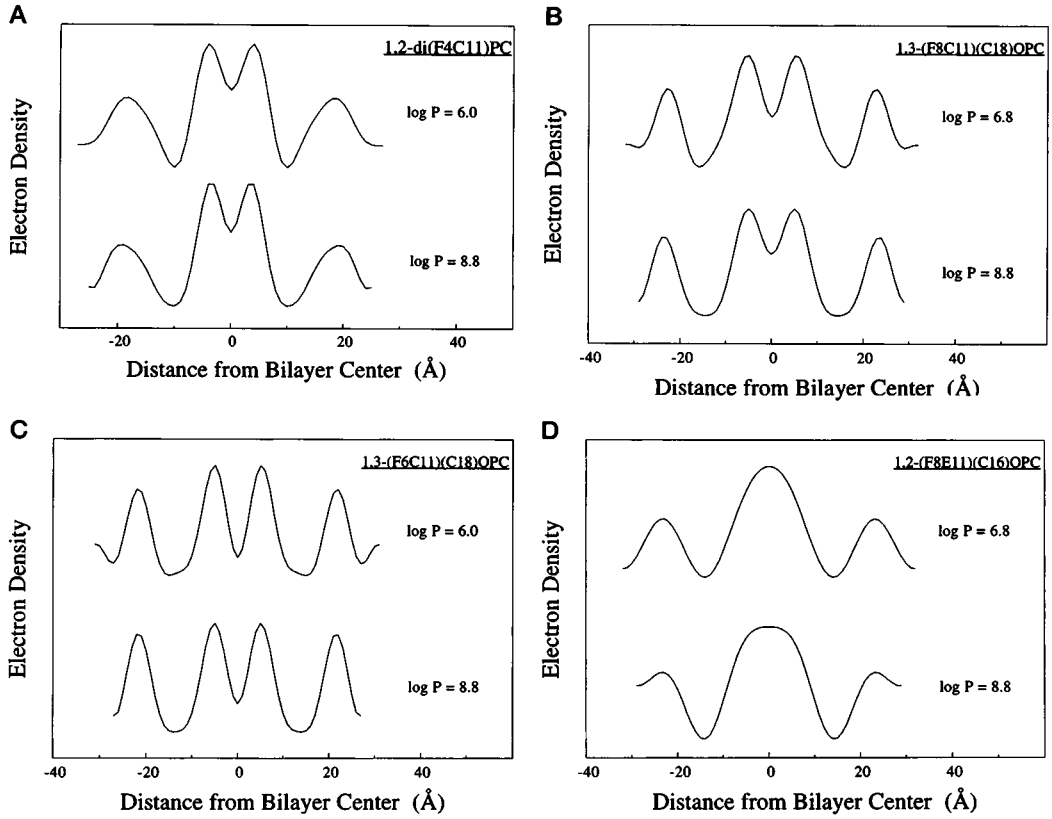


FIGURE 4 Electron density profiles of (*A*) 1,2-di(F4C11)PC, (*B*) 1,3-(F8C11)(C18)OPC, (*C*) 1,3-(F6C11)(C18)OPC, and (*D*) 1,2-(F8E11)(C16)OPC for applied pressures indicated in figure. Profiles are at a resolution ($d/2h_{max}$) of approximately 3 Å in *A*, 5 Å in *B* and *C*, and 7 Å in *D*.

density in the central region of the bilayer was significantly higher for the fluorinated 1,2-di(F4C11)PC than for the hydrocarbon lipid DPPC. Thus, the profile localizes the fluorines in the center of the 1,2-di(F4C11)PC bilayer.

Fig. 6 compares the profile of liquid-crystalline phase 1,3-(F8E11)(C16)OPC to the profiles of liquid-crystalline egg phosphatidylcholine. In this case the width of the bilayer was larger for 1,3-(F8E11)(C16)OPC. Again, there was clear evidence for the increased electron density in the bilayer center caused by the fluorines in 1,3-(F8E11)-(C16)OPC.

Fig. 7 compares the electron density profiles of three fluorinated lipids in the gel phase. As shown in Fig. 1, these

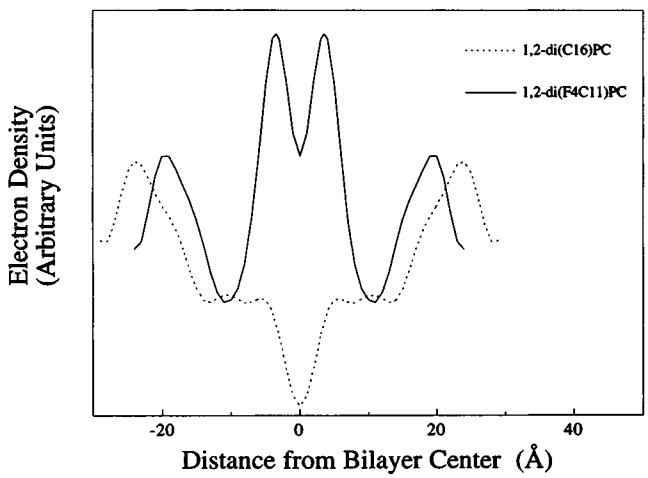


FIGURE 5 Electron density profiles of gel phase 1,2-di(F4C11)PC and gel phase 1,2-di(C16)PC (DPPC). The electron density profile of DPPC was calculated from the data of McIntosh and Simon (1993).

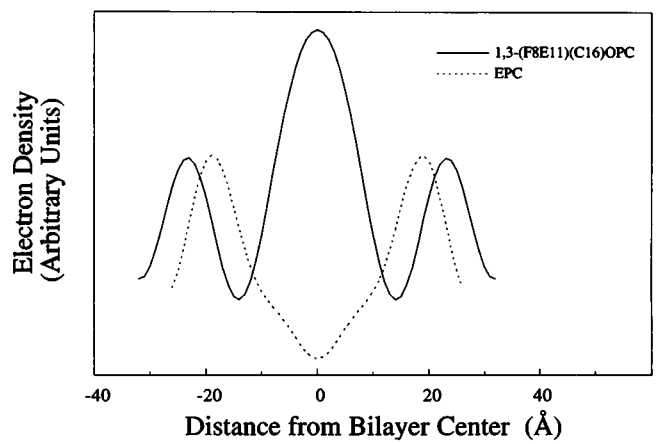


FIGURE 6 Electron density profiles of liquid-crystalline phase 1,3-(F8E11)(C16)PC and liquid-crystalline phase EPC at the same resolution of 7 Å. The profile of EPC was taken from McIntosh et al. (1987).

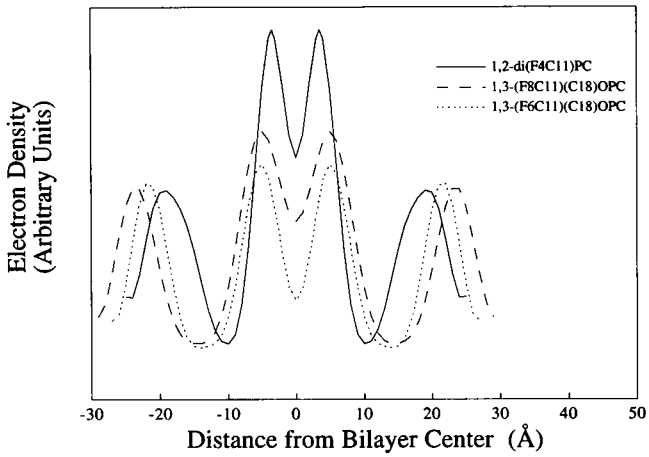


FIGURE 7 Electron density profiles of gel phase 1,2-di(F4C11)PC, 1,3-(F8C11)(C18)OPC, and 1,3-(F6C11)(C18)OPC.

lipids have different arrangements of the fluorines. 1,2-di(F4C11)PC has a total of 18 fluorine atoms, with nine on each chain; 1,3-(F8C11)(C18)OPC has 17 fluorine atoms, all on one chain; and 1,3-(F6C11)(C18)OPC has 13 fluorines, all on one chain. Several points should be noted. As expected, the shapes of the central regions of the electron density profiles were different for the three lipids. The high-density peaks in the center of the bilayer were higher and narrower for 1,2-di(F4C11)PC than for the other lipids. This is consistent with the distribution of fluorines being on the terminal regions of both alkyl chains and with the shorter fluorinated tail length for 1,2-di(F4C11)PC. The high-density region in the bilayer center was broader and higher for 1,3-(F8C11)(C18)OPC than for 1,3-(F6C11)-(C18)OPC, consistent with the larger number of fluorines that extend farther up the alkyl chain in 1,3-(F8C11)-(C18)OPC (Fig. 1). Moreover, $d_{pp}$ was largest for 1,3-(F8C11)(C18)OPC and smallest for 1,2-di(F4C11)PC. This can be explained by two factors. First, 1,3-(F8C11)-(C18)OPC has a larger number of carbons in its alkyl chains, and second, the mixture of broad and sharp wide-angle reflections (Table 1) indicates that the chains were more highly tilted for 1,2-di(F4C11)PC.

The electron density profiles allow us to estimate the bilayer thickness ($d_b$) and fluid layer thickness ($d_f$) for each applied osmotic pressure. As noted previously (McIntosh and Simon, 1986, 1993; McIntosh et al., 1992), the definition of the lipid/water interface is somewhat arbitrary, because the bilayer surface is rough and water penetrates into the headgroup region of the bilayer (Griffith et al., 1974; Worcester and Franks, 1976; Simon and McIntosh, 1986). In this paper, to facilitate comparison with our previous work on bilayers with hydrocarbon chains, we again operationally define the bilayer width as the total physical thickness of the bilayer, assuming that the conformation of the phosphorylcholine headgroup in fluorinated PC bilayers is the same as it is in single crystals of phosphatidylcholine (Pearson and Pascher, 1979). In that case the high-density headgroup peak would be located between the phosphate group and the glycerol backbone. We assume that the phosphorylcholine group is, on average, oriented approximately parallel to the bilayer plane, so that the edge of the bilayer lies about 5 Å outward from the center of the high-density peaks in the electron density profiles at 5- to 7-Å resolution (McIntosh and Simon, 1986; McIntosh et al., 1987, 1989a, 1992). Therefore, for each osmotic pressure we calculate the bilayer thickness as $d_b = d_{pp} + 10$ Å. We note that the small differences in resolution for the various fluorinated lipids can make a difference of about $\pm 1$ Å in these estimates of $d_b$. The distance between bilayer surfaces is calculated from $d_f = d - d_b$ (McIntosh and Simon, 1986, 1993; McIntosh et al., 1992).

Using this definition of the lipid/water interface, we plot in Fig. 8 the logarithm of applied osmotic pressure (log $P$) versus $d_f$ for the seven fluorinated lipids. The pressure-distance data were similar for the seven lipids in several respects. For all lipids $d_f$ decreased with increasing applied pressure. Furthermore, for fluid spaces of 4 Å $< d_f <$ 8 Å, the pressure-distance data were similar for all of the lipids. In this distance range, the log $P$ versus $d_f$ data could be fit to a straight line ($R^2 > 0.94$ in all cases, except for 1,3-(F8C11)(C18)OPC, where only a few data points were collected). This means that over this range of fluid spacings the total pressure decayed exponentially with increasing fluid space. For all fluorinated lipids the values for the exponential decay length were quite similar ($\lambda = 1.5 \pm 0.2$ Å). The magnitudes ($P_o$) of this exponential pressure (obtained by extrapolation to $d_f = 0$ Å) are given in Table 1.

For $d_f < 4$ Å and $d_f > 8$ Å, there were distinct differences among the lipids. In particular, for $d_f > 8$ Å, at low applied pressures, the pressure-distance curve extended to significantly larger values of $d_f$ for liquid-crystalline phase 1,2-

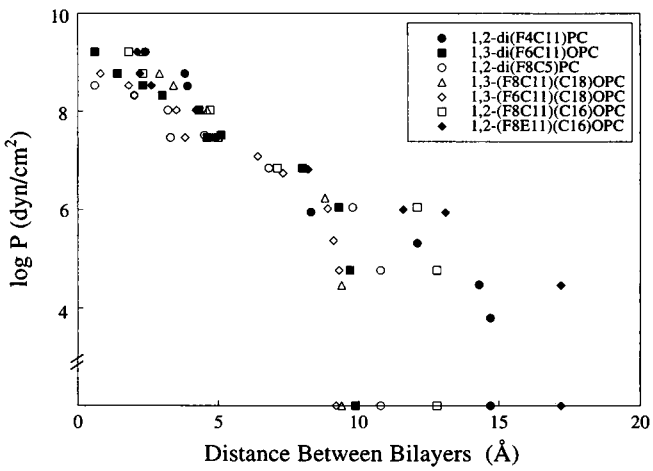


FIGURE 8 Plot of the logarithm of applied pressure (log $P$) versus the distance between apposing bilayers ($d_f$) for 1,2-di(F4C11)PC, 1,3-di-(F6C11)OPC, 1,2-di(F8C5)PC, 1,3-(F8C11)(C18)OPC, 1,3-(F6C11)-(C18)OPC, and 1,2-(F8C11)(C16)OPC in the gel phase, and 1,2-(F8E11)-(C16)OPC in the liquid-crystalline phase. The equilibrium fluid spaces are given on the $x$ axis.

(F8E11)(C16)OPC than for gel phase 1,3-di(F6C11)OPC, 1,2-di(F8C5)PC, or 1,3-(F8C11)(C18)PC. The gel phase lipids 1,2-di(F4C11)PC and 1,2-(F8C11)(C16)OPC were between these extreme cases. These differences in the range of the pressure can most easily be seen by noting the differences in the equilibrium fluid separations ($d_{fe}$) at zero applied pressures (denoted by the data points on the $x$ axis and collected in Table 1).

### Dipole potential

The measured dipole potentials for the fluorinated lipids, liquid-crystalline phase egg yolk phosphatidylcholine (EPC), and gel phase 1,2-di(C16)PC (DPPC) (taken from Simon and McIntosh, 1989) are shown in Table 1. All of the fluorinated lipids gave negative dipole potentials, ranging from −680 mV for 1,2-di(F8C5)PC to −184 mV for 1,3-(F6C11)(C18)OPC. These values of $V$ can be contrasted to the large positive values of $V$ for phosphatidylcholines with hydrocarbon chains, for example, +415 mV for EPC and +575 mV for 1,2-di(C16)PC (Table 1).

### Binding of hydrophobic ions

Fig. 9 shows the steady-state changes in dipole potential, $\Delta V$, measured after injection of tetraphenylboron ($TPB^-$) into the subphase below monolayers of EPC ($V$ = 415 mV) and 1,2-(F8E11)(C16)OPC ($V$ = −485 mV). The changes in the dipole potential plotted versus log{$TPB^-$} decreased monotonically for both lipids from $10^{-8}$ to $10^{-4}$ M. For EPC monolayers the changes in dipole potential were similar to those obtained for monolayers of bacterial phosphatidylethanolamine over a subphase containing 1.0 M NaCl (Andersen et al., 1978). For the range $10^{-7}$ to $10^{-4}$ M $TPB^-$, the slopes of the data in Fig. 9 ($\partial\Delta V/\partial\log\{TPB^-\}$) were −66 mV/10-fold change in {$TPB^-$} for EPC and −26 mV/10-fold change in {$TPB^-$} for 1,2-(F8E11)(C16)OPC.

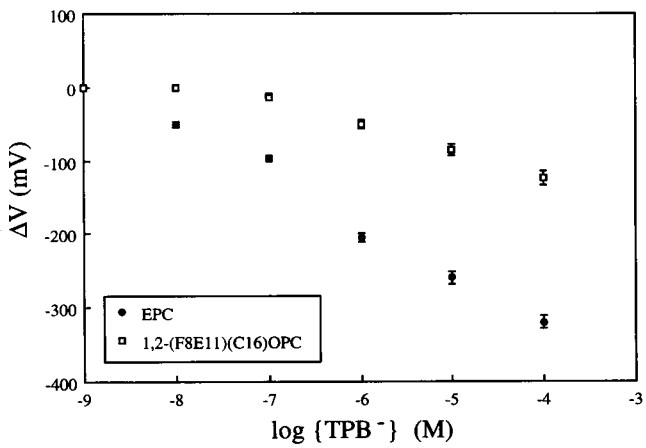


FIGURE 9 The change in dipole potential ($\Delta V$) upon the binding of tetraphenylboron ($TPB^-$) to monolayers of EPC and 1,3-(F8E11)(C18)OPC.

## DISCUSSION

The data presented in this paper provide information on the structure, interbilayer pressures, dipole potentials, and hydrophobic ion binding for membranes composed of various fluorocarbon/fluorocarbon and mixed fluorocarbon/hydrocarbon ester- and ether-connected glycerophosphocholines.

### Structure

The wide-angle (Table 1) and low-angle x-ray diffraction data (Figs. 2–7) show that all of these fluoroalkylated phospholipids form multilayered lipid bilayer structures in excess buffer. However, the data analysis indicates several significant structural differences between these highly fluorinated bilayers and phosphatidylcholine bilayers with hydrocarbon chains. First, in both gel and liquid-crystalline bilayers, the wide-angle spacings are larger for the fluorine-modified glycerophosphocholines than for analogous hydrocarbon phosphatidylcholines (Table 1). This indicates that in both the gel and liquid-crystalline phases the interchain separation is greater for the fluoroalkylated lipids than for conventional PCs with hydrocarbon chains. This is related to the greater size of a fully extended alkyl chain of $CF_2$ groups (cross-sectional area of about 30 Å$^2$) compared to that of a gel phase chain of $CH_2$ (cross-sectional area of about 20 Å$^2$) (Bunn and Howells, 1954), because of the larger radius of the fluorine atom (van der Waals radius of 1.35 Å) compared to that of the hydrogen atom (1.2 Å), and because the C-F bond length is about 0.25 Å longer than the C-H bond length. The greater interchain separation for the fluoroalkylated lipids can also be related to the smaller fluorocarbon/fluorocarbon or fluorocarbon/hydrocarbon chain-chain interactions compared to hydrocarbon/hydrocarbon interactions (Mukerjee and Handa, 1981). Second, both the wide-angle data (Table 1) and the electron density profiles (Fig. 5) indicate that for 1,2-di(F4C11)PC the fluoroalkyl chains must be tilted with respect to the bilayer normal. That is, a mixture of sharp and broad wide-angle reflections, such as observed for 1,2-di(F4C11)PC, is typical of lipids with tilted chains (McIntosh, 1980; Tardieu et al., 1973; Tristram-Nagle et al., 1993). Moreover, the electron density profiles (Figs. 4 *A* and 5 and Table 1) show a very narrow bilayer width for 1,2-di(F4C11)PC, consistent with highly tilted chains. Third, both the wide-angle data and the electron density profiles indicate that there is less chain tilt in 1,3-(F8C11)(C18)OPC and 1,3-(F6C11)(C18)OPC than in 1,2-di(F4C11)PC. The single, sharp wide-angle reflection is characteristic of gel phase bilayers with hydrocarbon chains that are approximately perpendicular to the plane of the bilayer (Tardieu et al., 1973; McIntosh, 1980), and the headgroup peak separation ($d_{pp}$) for both 1,3-(F8C11)(C18)OPC and 1,3-(F6C11)(C18)OPC is considerably greater than that of 1,2-di(C16)PC (Fig. 7, Table 1). Fourth, the presence of a large trough in the geometric center of each electron density profile and the values of the headgroup peak separations ($d_{pp}$, Table 1) for the gel phase ether-linked and 1,3-isomers indicate that these fluorinated glycerophosphocholines do not form interdigitated lamellar gel

phases such as those formed by hydrocarbon ether-connected analogs (Ruocco et al., 1985; Kim et al., 1987; Haas et al., 1990) or hydrocarbon ester-connected 1,3-isomers (Serrallach et al., 1983). The presence of deep electron density dips in the center of the bilayer means that the terminal $CF_3$ and $CH_3$ are localized in the center of the bilayer and the values of $d_{pp}$ for the ether-linked and 1,3-isomers (Table 1) are larger than those expected for an interdigitated phase (30 Å for ether-linked dihexadecylphosphatidylcholine) (Kim et al., 1987). Fifth, and most importantly for the analysis that follows, the electron density profiles show that the fluorinated regions of the alkyl chains are localized in the bilayer center, supporting the schematic structural depictions given by Santaella et al. (1993) and Frézard et al. (1994a). For a gel phase composed of both fluorocarbon/fluorocarbon phospholipids, 2-di(F4C11)PC and mixed fluorocarbon/hydrocarbon phospholipids, 3-(F6C11)-(C18)OPC and 1,3-(F8C11)(C18)OPC, the positions and widths of the high-density peaks in the center of the profiles (Figs. 4, 5, 7) are consistent with the expected positions of the fluorines in the molecules (Fig. 1) in well-ordered lipid bilayers with stiff alkyl chains. In particular, for 1,2-di(F4C11)PC the extremely high and narrow density peaks in the center of the bilayer show that the fluorines of the terminal four carbons are localized in the center of the bilayer. The distinct terminal dip in the profile, indicative of localized $CF_3$ groups, is another indication of the orderly packing in the bilayer center (Fig. 7). In the case of 1,3-(F8C11)(C18)OPC and 1,3-(F6C11)-(C18)OPC, the central electron density peaks due to the fluorines are wider and not as high. For these bilayers the fluorines extend farther from the bilayer center, because the terminal eight and six carbons of one alkyl chain are fluorinated. In the case of liquid-crystalline phase 1,2-(F8E11)(C16)OPC, the central fluorine peaks are not as sharp (Figs. 4 *D* and 6), indicating a more fluid bilayer interior.

## Dipole potentials

The physical origin of the dipole potential for monolayers at the air-water interface, as well as its relevance to dipole potentials in bilayers (see below), has been a matter of controversy and discussion for a number of years (Vogel and Möbius, 1988; Simon and McIntosh, 1989; Taylor et al., 1990; Mingins et al., 1992; Brockman, 1994). Although $V$ has not previously been measured for fluorinated phospholipids, previous monolayer experiments have shown, for example, that for stearic acid the substitution of the terminal $-CH_3$ moiety with a $-CF_3$ moiety changes $V$ from +275 mV to −915 mV (Vogel and Möbius, 1988). Measurements on phospholipids with hydrocarbon chains show that $V$ is lowered by as much as 100 mV by substituting carbonyl groups with ether groups (Gawrisch et al., 1992), moving an acyl chain from the 2 to the 3 position (Smaby and Brockman, 1990), or increasing the area per lipid molecule (Smaby and Brockman, 1990).

Our measured dipole potentials (Table 1) show that fluorinated PCs exhibit many of these same features. That is, lipids with terminal $-CF_3$ moieties in both chains have large negative dipole potentials ($V \approx -600$ mV), whereas DPPC monolayers with terminal $-CH_3$ groups in both chains have large positive dipole potentials (+575 mV). PCs with one fluoroalkylated and one hydrocarbon chain have relatively small negative dipole potentials. The dipole potential is less sensitive to the number of $CF_3$ groups in the alkyl chain(s), differing by about 40 mV with the addition of two $CF_2$ groups in one chain, from $V = -184$ mV for 1,3-(F6C11)(C18)OPC to $V = -220$ mV for 1,3-(F8C11)-(C18)OPC. Thus these data indicate that the terminal $CF_3$ group has a larger influence on $V$ than does the symmetric $CF_2$ groups and that the large $CF_3$ dipole markedly contributes to $V$ of monolayers at air-water interfaces. This is further confirmed by the larger magnitude of $V$ found for 1,2-di(F4C11)PC compared to that of 1,2-(F8C11)-(C16)OPC. These two compounds possess the same number of fluorinated carbons (eight), but the former has two $CF_3$ groups, whereas the latter contains one $CF_3$ group. Altering the position of the chains on the glycerol backbone from a 1,2 isomer to a 1,3 isomer changes $V$ by about 200 mV to −445 mV for 1,2-(F8C11)(C16)OPC, and $V = -220$ mV for 1,3-(F8C11)(C18)OPC. However, changing the chain linkage from ester to ether seems to have relatively little effect on dipole potential in the fluorinated series (the increase of about 200 mV from 1,2-di(F8C5)PC to 1,3-di(F6C11)OPC corresponds to the increase found when going from a 1,2 to a 1,3 isomer). The dipole potential is larger in magnitude for 1,2-(F8E11)(C16)OPC than for 1,2-(F8C11)(C16)OPC. In this case the double bond in 1,2-(F8E11)(C16)OPC could modify the orientation of the fluorine dipoles.

## Interbilayer repulsive pressures

We consider the pressure-distance data (Fig. 8) in terms of the repulsive pressures thought to be present between hydrocarbon phosphatidylcholine bilayers. There are two general classes of short-range pressures between zwitterionic phosphatidylcholine lipid bilayers: the hydration pressure, due to partial polarization or H-bond reorganization of water by the hydrophilic bilayer surface (Marcelja and Radic, 1976; LeNeveu et al., 1977; Parsegian et al., 1979; Gruen and Marcelja, 1983; Attard and Batchelor, 1988; McIntosh and Simon, 1986, 1993; Rand and Parsegian, 1989), and entropic (steric) pressures, due to headgroup overlap at small fluid spacings (McIntosh et al., 1987, 1989a), protrusions of individual or several lipid molecules (Israelachvili and Wennerstrom, 1990, 1992, 1996; Lipowsky and Grotehans, 1993), or thermally induced bilayer undulations or fluctuations (Harbich and Helfrich, 1984; Helfrich and Servuss, 1984; Evans and Parsegian, 1986; Evans, 1991). For phosphatidylcholine bilayers at relatively large fluid separations, there is agreement that the only attractive pressure is the van der Waals pressure (LeNeveu et al., 1977; Marra and Israelachvili, 1985). Because it is

difficult to separate the contributions of the various types of repulsive pressures in fluid bilayers, we (McIntosh and Simon, 1993) have previously measured the pressure-fluid spacing relations for DPPC bilayers in the subgel phase. In the subgel phase the acyl chains are crystalline, and thus all out-of plane protrusions and fluctuations are significantly reduced, so that the primary repulsive pressure is the hydration pressure (McIntosh and Simon, 1993). In the following analysis we compare the pressure-distance data from fluorinated lipids and subgel phase DPPC.

Fig. 10 compares the pressure-distance data for the fluorinated lipids in the gel phase with previously recorded data from gel and subgel phases of the hydrocarbon lipid DPPC (McIntosh and Simon, 1993), and Fig. 11 shows the logarithm of the applied pressure versus $d_f$ for liquid crystalline 1,2-(F8E11)(C16)OPC, subgel DPPC, and two liquid-crystalline PCs with hydrocarbon chains, phosphatidylcholine isolated from egg yolks (EPC) and the polyunsaturated synthetic PC 1,2-diarachidonylphosphatidylcholine (DAPC). EPC is chosen for comparison because it is one of the most commonly studied lipids and has a hydrocarbon chain composition similar to typical membrane phospholipids. DAPC, with four double bonds in each chain, has a smaller bending modulus than EPC and therefore has a larger repulsive undulation pressure than EPC (McIntosh et al., 1995).

To simplify the presentation, we discuss the pressure-distance relations in terms of three somewhat arbitrarily defined distance ranges: "small" ($d_f < 4$ Å), "intermediate" (4 Å $< d_f <$ 8 Å), and "large" interbilayer separations ($d_f >$ 8 Å).

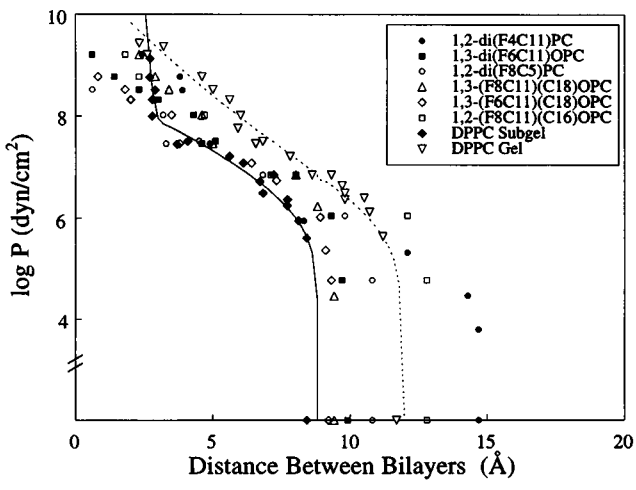


FIGURE 10 Plot of the logarithm of applied pressure (log $P$) versus the distance between apposing bilayers ($d_f$) for 1,2-di(F4C11)PC, 1,3-di(F6C11)OPC, 1,2-di(F8C5)PC, 1,3-(F8C11)(C18)OPC, 1,3-(F6C11)-(C18)OPC, and 1,2-(F8C11)(C16)OPC in the gel phase and fully hydrogenated DPPC in the gel and subgel phases (taken from McIntosh and Simon, 1993). The equilibrium fluid spaces are given on the $x$ axis. The dotted and solid lines represent least-squares fits to the DPPC gel and subgel phase data (McIntosh and Simon, 1993).

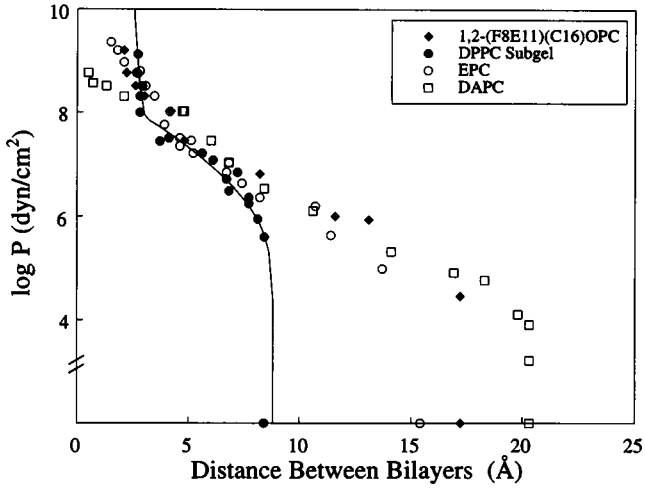


FIGURE 11 Plot of the logarithm of applied pressure (log $P$) versus the distance between apposing bilayers ($d_f$) for 1,2-(F8E11)(C16)OPC in the liquid-crystalline phase and three lipids with hydrocarbon chains: DPPC in the subgel phase, EPC in the liquid-crystalline phase, and DAPC in the liquid-crystalline phase. The equilibrium fluid spaces are given on the $x$ axis. Data for DPPC and EPC are from McIntosh and Simon (1993) and data for DAPC are from McIntosh et al. (1995). The solid line represents a least-squares fit to the DPPC subgel phase data (McIntosh and Simon, 1993).

## Very small interbilayer separations

At small fluid spacings ($d_f < 4$ Å) the pressure-distance data differ for the various fluorinated lipids (Fig. 8). We have previously shown that the repulsive pressure for $d_f < 4$ Å is primarily due to steric interactions between lipid headgroups from apposing bilayers, and the magnitude of this steric pressure depends on the volume fraction of PC headgroups at the interface (McIntosh et al., 1987, 1989a). Therefore, as seen in Fig. 11, bilayers with small areas per molecule, such as subgel phase DPPC, have larger repulsive pressures for $d_f < 4$ Å than do bilayers with large area per molecule, such as DAPC. Most of the fluorinated lipids have repulsive pressures for $d_f < 4$ Å that are intermediate in magnitude between those of subgel DPPC and DAPC. This is consistent with recent surface pressure-area isotherms for some of the fluorinated PCs (Rolland et al., 1996), which show that their areas per molecule at the collapse pressure (58 Å$^2$ for 1, 2-di(F4C11)PC) are greater than those of DPPC (about 40 Å$^2$; Rolland et al., 1996), but less than that of polyunsaturated DAPC (about 76 Å$^2$; Smaby et al., 1994).

Molecular protrusions (Israelachvili and Wennerstrom, 1990, 1992) might also contribute to the short-range repulsive pressure. However, given that the protrusion pressure depends on the energy to transfer a acyl chain in the bilayer into water, we would expect molecular protrusions to be reduced for fluorinated lipids compared to hydrocarbon lipids, because the free energy of transfer of a $CF_2$ from either a perfluorocarbon or hydrocarbon interface into water (1210 cal/mol) is greater than the free energy of transferring a $CH_2$ group from oil to water (820 cal/mol) (Mukerjee and Handa, 1981). Moreover, protrusions of fluorinated lipids in

the bilayer would require a mixing of the fluorocarbons at the end of the chain with the hydrocarbons near the interfacial region, which would also be energetically unfavorable (Hildebrand et al., 1970).

### Intermediate separations

For 4 Å $< d_f <$ 8 Å, the pressure distance data for all of the fluorinated lipids can be described by single exponential decay functions with similar decay lengths ($\lambda \approx 1.5 \pm 0.2$ Å) and the magnitudes ($P_o$) given in Table 1. In this distance regime for the gel and subgel phases it has been argued that the dominant repulsive pressure is the hydration pressure (McIntosh and Simon, 1993; Simon et al., 1995). Therefore these data indicate that the underlying hydration pressure is similar for bilayers formed from analogous hydrocarbon and fluorocarbon phospholipids. The data also imply that the fluorines located deep in the bilayer interior have relatively small effects on the decay length, a parameter thought to characterize the decay of solvent polarization (Marcelja and Radic, 1976; Eβmann et al., 1995). However, the presence of the fluorines has a marked impact on the measured dipole potentials (Table 1).

The reason for considering the dipole potential ($V$) in our analysis is that, as noted above, the magnitudes of the hydration pressure (Marcelja and Radic, 1976; Parsegian et al., 1979) and $V$ (Simon and McIntosh, 1989; Eβmann et al., 1995; Chiu et al., 1995) are thought to depend, at least in part, on the organization of interfacial water (see Appendix). Moreover, Cevc and Marsh (1985) have shown theoretically that the hydration pressure ($P_h$) can be written as

$$P_h = 2\chi \cdot (\Psi_h/\lambda)^2 \exp(-d_f/\lambda), \quad (3)$$

where $\Psi_h$ is the hydration potential and $\chi$ is the orientational susceptibility of the solvent. Simon and McIntosh (1989) have argued that $V$ measured from monolayers at the air-water interface provides an experimental estimate for the hydration potential, so that

$$P_h = 2\chi \cdot (V/\lambda)^2 \exp(-d_f/\lambda), \quad (4)$$

where the magnitude of the hydration pressure $P_o = 2\chi \cdot (V/\lambda)^2$. For a variety of hydrocarbon PCs it has been shown experimentally that the magnitude of the hydration pressure is indeed predicted by the expression $2\chi \cdot (V/\lambda)^2$. That is, with hydrocarbon lipids Simon et al. (Simon and McIntosh, 1989; Simon et al., 1991, 1992) and McIntosh et al. (1992) observed the correlation given in Eq. 4 between the hydration pressure and $V$ measured in monolayers with different 1) lipid headgroup structures, 2) lipid phases, and 3) solvents in the subphase below the monolayer.

Because according to Eq. 4 the magnitude of $P_h$ is proportional to the square of the dipole potential, bilayers with both large positive and large negative dipole potentials should have similar hydration pressures. However, for the fluorinated lipids the magnitude ($P_o$) of the exponential pressure observed for 4 Å $< d_f <$ 8 Å does not seem to be closely related to the square of the dipole potential measured with monolayers (Table 1). There are several possible factors that could contribute to these observed differences. First, although the diffraction data for all of the hydrocarbon lipids were collected at the same resolution (Simon and McIntosh, 1989; Simon et al., 1991, 1992), the diffraction data from each of the fluorinated lipids were collected at slightly different resolutions. As noted in the Results, this can lead to differences of about ±1 Å in the estimated bilayer thicknesses, which can give rise to uncertainties as large as a factor of 2 in the estimates of $P_o$. Second, although we have presented evidence that the hydration pressure is the dominant repulsive pressure for 4 Å $< d_f <$ 8 Å (McIntosh and Simon, 1993; Simon et al., 1995), entropic pressures also contribute to the measured repulsive pressure in this range of fluid spacings, particularly in the case of liquid-crystalline bilayers. Third, despite the experimental agreement with Eq. 4 for hydrocarbon lipids (Simon and McIntosh, 1989; Simon et al., 1991, 1992), the possibility should be considered that the theoretical analysis of the hydration pressure (Eq. 3) is invalid. However, we note that although more sophisticated theoretical models of the hydration pressure (with more unknown variables) have subsequently been developed (Kornyshev and Leikin, 1989; Cevc, 1991), the essentials of the original derivation leading to Eq. 4 seem to be preserved. Moreover, several molecular dynamics simulations of lipid water systems show that the electric fields arising from the partial charges and dipoles of the lipid headgroup are compensated by the solvent dipoles, the polarization of which decays in an approximately exponential manner from the apposing surfaces (Marrink et al., 1993; Zhou and Schulten, 1995; Chiu et al., 1995; Eβmann et al., 1995). Fourth, in Eq. 3 the substitution of $V$ for the hydration potential ($\Psi_h$) could be invalid. That is, the measurement of $V$ for monolayers at the air-water interface might not accurately reflect the value of either $\Psi_h$ or $V$ for bilayers. In the case of fluorinated lipids a potentially important factor is that dipolar fields decrease with increasing distance from dipoles located near the bilayer center and would be attenuated both at the hydrocarbon-water (high dielectric) interface and across the 10-Å width of the lipid headgroup region. Therefore, the large fields arising from the $CF_3$ dipoles in the center of the bilayer (which, as described above, make large contributions to $V$ measured in monolayers) might not significantly modify the orientation of interlamellar water molecules. This fourth possibility would also be relevant for fluorinated lipids if the differences in $V$ measured for monolayers and bilayers were larger for fluorinated lipids than for hydrocarbon lipids. We now explore this last possibility in detail.

For a variety of single and double-chained zwitterionic hydrocarbon lipids, the values of $V$ measured in monolayers at the air-water interface are about 150 mV larger than those measured in bilayers (Latorre and Hall, 1976; Reyes et al., 1983; Simon and McIntosh, 1989; Gawrisch et al., 1992; Brockman, 1994). However, the changes in $V$ due to the

additions of phloretin or some phloretin analogs are virtually identical, as measured in monolayers and planar bilayers (Reyes et al., 1983). This implies that, although the magnitude of $V$ is different as measured in monolayers or bilayers, changes in dipole potential are similar with the two techniques. There are several possible reasons for the observed difference in magnitude of $V$ measured in monolayers and bilayers. First, the measurements are based on entirely different principles and therefore might not be expected to give the same values (Simon and McIntosh, 1989). Brockman (1994) argues that for neutral phospholipids the difference likely reflects the contribution to $V$ measured in monolayers that arises from the reorganization of interfacial water occurring during lipid spreading in monolayers. In contrast, Vogel and Möbius (1988) argue that the terminal methyl group makes the largest contribution to $V$ measured in monolayers. We note that in bilayers the terminal $CH_3$ (or $CF_3$) groups from apposing monolayers intercalate (Huang and Li, 1996). To reduce their free energy, these intercalated terminal groups should partially align with their dipoles pointing in opposite directions. This would result in a partial cancellation of their dipole moments to $V$ measured in bilayers, whereas in monolayers at the air-water interface the contribution of the $CH_3$ dipoles would be uncompensated. Similar arguments can be made for fluorinated lipids with one hydrocarbon and one fluorinated chain.

The relatively small difference (about 150 mV out of 415 mV for EPC) in $V$ for hydrocarbon lipids measured between monolayers and bilayers (Reyes et al., 1983) apparently does not appreciably affect the correlation between $P_o$ and $2\chi \cdot (V/\lambda)^2$ observed for hydrocarbon lipids (Simon and McIntosh, 1989; Simon et al., 1991, 1992). Indeed, Brockman (1994) reported for hydrocarbon lipids that taking this 150-mV difference into account brings the calculated values more into line with measured values, but does not make them identical. However, because the dipole moment of $CF_3$ is larger than that of $CH_3$ (Vogel and Möbius, 1988), the difference in $V$ measured between monolayers and bilayers would be expected to be larger for fluorinated lipids than for hydrocarbon lipids. If that were the case, for fluorinated lipids $V$ measured in monolayers would not be expected to correlate as well with the magnitude of the hydration pressure as given in Eq. 4. Specifically, it would be expected that $V$ would be lower in magnitude for fluorinated bilayers than for analogous hydrocarbon bilayers. In this regard, we do observe that $P_o$ for gel phase DPPC is greater than $P_o$ for the gel phase fluorinated lipids (Fig. 10 and Table 1).

Thus we argue that the poor correlation between $P_o$ and $2\chi \cdot (V/\lambda)^2$ for fluorinated lipids might be at least partially due to differences in $V$ measured for monolayers and bilayers.

## Large interbilayer separations

For $d_f > 8$ Å, the pressure-distance data are quite different for the various fluorinated lipids (Fig. 8). In particular, the pressure-distance data from the liquid-crystalline phase 1,2-(F8E11)(C16)OPC extend to much longer bilayer separations than do the data from the comparable gel phase mixed-chain lipids, 1,3-(F8C11)(C18)OPC and 1,3-(F6C11)(C18)OPC. In addition, the equilibrium fluid spacings are smaller for gel phase 1,2-di(F8C5)PC and 1,3-di(F6C11)OPC than for the liquid-crystalline lipids. This is almost certainly due to the presence of the repulsive undulation pressure in the liquid-crystalline fluorinated lipids. Liquid-crystalline bilayers are much more flexible than unrippled gel phase bilayers, and thermally induced bilayer undulations or fluctuations provide an additional repulsive pressure in liquid-crystalline bilayers (Helfrich, 1973; Helfrich and Servuss, 1984; Evans and Parsegian, 1986). Previous experiments (McIntosh and Simon, 1993; McIntosh et al., 1995) have shown that the undulation pressure extends the range of the total repulsive pressure in PCs with hydrocarbon chains. The same situation likely occurs for the fluorinated bilayers in the liquid-crystalline phase. Fig. 11 shows that, compared to the subgel phase, where the undulation pressure is extremely small (McIntosh and Simon, 1993), the pressure-distance data extend to much larger values of $d_f$ for liquid-crystalline 1,2-(F8E11)(C16)OPC, EPC, and DAPC. Previously we showed that the reason that DAPC has a larger equilibrium fluid spacing than EPC can be explained by DAPC having a larger undulation pressure by virtue of a smaller bending modulus (McIntosh and Simon, 1993). The observation that the equilibrium value of $d_f$ for 1,2-(F8E11)(C16)OPC is between those of EPC and DAPC predicts that the bending modulus and the undulation pressure for this fluorinated lipid are between the values for EPC and DAPC.

An alternative explanation for the relatively large equilibrium fluid space for 1,2-(F8E11)(C16)OPC is that the addition of large volume fractions of fluorine in the chain region of the bilayer could result in a reduction in the attractive van der Waals pressure by a reduction in the Hamaker coefficient. However, the Hamaker coefficient for polytetrafluoroethylene is $3.6 \times 10^{-14}$ ergs (Gingell and Parsegian, 1973), which is approximately the same magnitude as found for $n$-alkanes and lipid bilayers ($3–5 \times 10^{-14}$ ergs) (Parsegian and Ninham, 1969; Ninham and Parsegian, 1970; Israelachvili, 1985; Rand and Parsegian, 1989). Thus, to a first approximation, the addition of fluorines in the chain region of the bilayer should not markedly alter the attractive van der Waals interactions. It follows that the comparatively large equilibrium fluid spacing for 1,2-(F8E11)(C16)OPC (Fig. 11) must be due primarily to the presence of a repulsive undulation pressure rather than a reduction in the attractive van der Waals pressure.

Most of the gel phase fluorinated bilayers have equilibrium fluid spacings between that of subgel and gel phase DPPC (Fig. 10), consistent with the primary repulsive pressure being the hydration pressure. However, the equilibrium fluid separations for 1,2-di(F4C11)PC and 1,2-(F8C11)(C16)OPC are somewhat larger. In these cases we argue that the increased fluid spacing might be

due to the presence of an additional repulsive pressure arising from surface ripples. DPPC bilayers in rippled ($P\beta'$) lamellar phases have larger equilibrium fluid spaces than do gel phase DPPC bilayers in unrippled ($L\beta'$) phases (Janiak et al., 1976; Inoko and Mitsui, 1978). It has also been shown that inducing ripples in flat ($L\beta'$) bilayers by the addition of exogenous molecules also increases the fluid spacing (Simon and McIntosh, 1991). Needham and Evans (1988) showed that the ripples can be "pulled out" of single $P\beta'$ PC bilayers by applying a lateral tension. Our pressure-distance data for 1,2-di-(F4C11)OPC and 1,2-(F8C11)(C16)OPC were obtained at 12°C and 23°C, respectively, which are near the respective thermal pretransitions measured by DSC of 14°C (Santaella et al., 1994) and 32°C (Vierling et al., 1995). These pretransition peaks are a few degrees in width. Such peaks generally appear at lower temperatures in oriented multilayers and usually reflect a transition from an unrippled gel phase to a rippled $P\beta'$ phase (Janiak et al., 1976). Thus it is possible that at 12°C or 23°C, respectively, the 1,2-di(F4C11)PC and 1,2-(F8C11)(C16)OPC bilayers contain ripples and that these ripples give rise to a repulsive steric pressure. The application of a lateral tension via osmotic pressure would pull out these ripples and cause the pressure-distance curve for 1,2-di(F4C11)PC or 1,2-(F8C11)(C16)OPC to superimpose on that of the subgel phase DPPC at high applied pressures, as observed in Fig. 10.

### Binding of tetraphenylboron

The binding of the hydrophobic ion $TPB^-$ to membranes depends, along with other factors, on the membrane dipole potential (Honig et al., 1986). Because EPC and 1,2-(F8E11)(C16)OPC have different signs of dipole potential (Table 1), the binding of $TPB^-$ to monolayers of these lipids provides information regarding the propagation of the dipolar field into the interfacial region. The presence of fluorines in the chains reduces the change in dipole potential produced by $TPB^-$. That is, for $10^{-7}$ M to $10^{-4}$ M, the slopes of the data points in Fig. 9 ($\partial\Delta V/\partial\log\{TPB^-\}$) are quite different for EPC and 1,2-(F8E11)(C16)OPC, indicating that the binding of $TPB^-$ is different for the two lipids (Andersen, 1978). Because $TPB^-$ binds at the level of the hydrocarbon-water interface of the bilayer (Cafiso, 1995; Smejtek, 1995), this means that the electric field produced by the fluorines must extend at least to this location in the bilayer. The most likely reason for the decrease in slope is that the magnitude of the positive dipole potential in the PC headgroup region is reduced by the negative potential produced by the $CF_3$ and $CF_2$ dipoles.

### Relevance to drug delivery

The stability of liposomes in the blood is thought to involve the interaction of plasma proteins (usually negatively charged) with the bilayer (Semple et al., 1996). Because the electric field due to the fluorine dipoles extends to the bilayer headgroup region and modifies the binding of negatively charged hydrophobic ions (Fig. 9), we propose that the dipole potential of the fluorinated lipids reduces the binding of negatively charged serum proteins that partition into the interfacial region of the bilayer. This reduced protein binding could contribute to the extended stability and blood circulation time that has been observed for liposomes containing fluoroalkylated PCs (Santaella et al., 1993; Frézard et al., 1994a,b).

## APPENDIX: CONTRIBUTIONS OF HEADGROUP REGION TO DIPOLE POTENTIAL

Several pieces of evidence indicate that for phospholipids the dipole potential has large contributions from the dipoles of both lipid and water molecules in the lipid headgroup region. Analyses of molecular dynamics simulations of bilayers of phosphatidylcholine or phosphatidylethanolamine indicate that the dipole potential arises from dipoles of the lipid headgroups and the compensating polarized water molecules (Marrink et al., 1993; Zhou and Schulten, 1995; Chiu et al., 1995; Eβmann et al., 1995). Moreover, the shape of the potential energy barrier produced by the dipole field in hydrocarbon lipid bilayers indicates the importance of dipoles in the headgroup region. If the polar headgroups and associated waters were the principal moieties responsible for this potential, the shape of the energy barrier should be nearly trapezoidal. That is, the potential would rise from zero in the aqueous phases to a maximum at some point near the hydrocarbon-water interface and be nearly constant across the bilayer interior (Franklin and Cafiso, 1993). On the other hand, if the major energy barrier were primarily due to the terminal methyl groups, the barrier shape would be triangular, with its peak centered near the terminal methyl groups. Numerous experimental studies with bilayers indicate that the dipole potential barrier is approximately trapezoidal in shape (Latorre and Hall, 1976; Franklin and Cafiso, 1993). The most convincing evidence that the barrier shape is not triangular is the measurement of the dipole potential in asymmetrical planar lipid bilayers with both lipids containing hydrocarbon chains (Latorre and Hall, 1976). If the terminal methyl groups gave rise to the dominant energy barrier (i.e., triangular barrier), no changes in dipole potential should be observed between symmetrical and asymmetrical bilayers. However, changes in the dipole potential were measured in asymmetrical planar bilayers, and moreover, the magnitudes of these changes are consistent with the differences in the dipole potentials measured in monolayers of these two lipids at the air-water interfaces (Latorre and Hall, 1976). These data indicate that although the $CH_3$ groups contribute to $V$ measured in monolayers, their relative contribution to $V$ measured in hydrocarbon bilayers is small.

We thank Dr. V. A. Parsegian for helpful discussions concerning van der Waals interactions, Dr. Robert MacDonald for insights concerning dipole potentials, and Dr. Nam-Won Huh for assistance with the dipole potential measurements.

This work was supported by grant GM-27278 from the National Institutes of Health and by the CNRS of France.

## REFERENCES

Adam, N. K. 1968. The Physics and Chemistry of Surfaces. Dover Publications, New York.

Allen, T. M., C. Hansen, F. Martin, C. Redemann, and A. Yau-Young. 1991. Liposomes containing synthetic lipid derivatives of poly(ethyleneglycol) show prolonged circulation half-lives in vivo. *Biochim. Biophys. Acta.* 1066:29–36.

Andersen, O. S. 1978. Permeability Properties of Unmodified Lipid Membranes in Membrane Transport in Biology. Springer-Verlag, Berlin.

Andersen, O. S., S. Feldberg, H. Nakadomari, S. Levy, and S. McLaughlin. 1978. Electrostatic interactions among hydrophobic ions in lipid bilayer membranes. *Biophys. J.* 21:35–70.

Attard, P., and M. T. Batchelor. 1988. A mechanism for the hydration force demonstrated in a model system. *Chem. Phys. Lett.* 149:206–211.

Blaurock, A. E., and C. R. Worthington. 1966. Treatment of low angle X-ray data from planar and concentric multilayered structures. *Biophys. J.* 6:305–312.

Blume, G., and G. Cevc. 1990. Liposomes for the sustained drug release in vivo. *Biochim. Biophys. Acta.* 1029:91–97.

Brockman, H. L. 1994. Dipole potentials of lipid membranes. *Chem. Phys. Lipids.* 73:57–79.

Bunn, C. W., and E. R. Howells. 1954. Structures of molecules and crystals of fluorocarbons. *Nature.* 174:549–551.

Cafiso, D. S. 1995. Influence of charges and dipoles on macromolecular adsorption and permeability. *In* Permeability and Stability of Lipid Bilayers. E. A. Disalvo and S. A. Simon, editors. CRC Press, Boca Raton, FL. 179–196.

Cevc, G. 1991. Hydration force and the interfacial structure of the polar surface. *J. Chem. Soc. Faraday Trans.* 87:2333–2379.

Cevc, G., and D. Marsh. 1985. Hydration of noncharged lipid bilayer membranes. Theory and experiments with phosphatidylethanolamine. *Biophys. J.* 47:21–32.

Chiu, S.-W., M. Clark, V. Balaji, S. Subramaniam, H. L. Scott, and E. Jakobsson. 1995. Incorporation of surface tension into molecular dynamics simulation an interface: a fluid phase lipid bilayer. *Biophys. J.* 69:1230–1245.

Eβmann, U., L. Perera, and M. L. Berkowitz. 1995. Simulation of DPPC membranes in subgel and liquid crystalline phase. *Langmuir.* 11: 4519–4531.

Evans, E. 1991. Entropy-driven tension in vesicle membranes and unbinding of adherent vesicles. *Langmuir.* 7:1900–1908.

Evans, E. A., and V. A. Parsegian. 1986. Thermal-mechanical fluctuations enhance repulsion between bimolecular layers. *Proc. Natl. Acad. Sci. USA.* 83:7132–7136.

Franklin, J. C., and D. S. Cafiso. 1993. Internal electrostatic potentials in bilayers: measuring and controlling dipole potentials in lipid vesicles. *Biophys. J.* 68:289–299.

Franks, N. P. 1976. Structural analysis of hydrated egg lecithin and cholesterol bilayers. I. X-ray diffraction. *J. Mol. Biol.* 100:345–358.

Frézard, F., C. Santaella, M.-J. Montisci, P. Vierling, and J. G. Riess. 1994a. Fluorinated phosphatidylcholine-based liposomes: $H^+/Na^+$ permeability, active doxorubicin encapsulation and stability in human serum. *Biochim. Biophys. Acta.* 1194:61–68.

Frézard, F., C. Santaella, P. Vierling, and J. G. Riess. 1994b. Permeability and stability in buffer and in human serum of fluorinated phospholipid-based liposomes. *Biochim. Biophys. Acta.* 1192:61–70.

Gawrisch, K., D. Ruston, J. Zimmerberg, V. A. Parsegian, R. P. Rand, and N. Fuller. 1992. Membrane dipole potentials, hydration forces, and the ordering of water at membrane surfaces. *Biophys. J.* 61:1213–1223.

Gingell, D., and V. A. Parsegian. 1973. Prediction of van der Waals interactions between plastics in water using the Lifshitz theory. *J. Colloid Interface Sci.* 44:456–463.

Griffith, O. H., P. J. Dehlinger, and S. P. Van. 1974. Shape of the hydrophobic barrier of phospholipid bilayers: evidence for water penetration in biological membranes. *J. Membr. Biol.* 15:159–192.

Gruen, D. W. R., and S. Marcelja. 1983. Spatially varying polarization in water. *J. Chem. Soc. Faraday Trans. 2.* 79:225–242.

Haas, N. S., P. K. Spirada, and G. G. Shipley. 1990. Effect of chain linkage on the structure of phosphatidylcholine bilayers. *Biophys. J.* 57: 117–124.

Harbich, W., and W. Helfrich. 1984. The swelling of egg lecithin in water. *Chem. Phys. Lipids.* 36:39–63.

Helfrich, W. 1973. Elastic properties of lipid bilayers: theory and possible experiments. *Z. Naturforsch.* 28C:693–703.

Helfrich, W., and R.-M. Servuss. 1984. Undulations, steric interactions and cohesion of fluid membranes. *Il Nuovo Cimento.* 3:137–151.

Herbette, L., J. Marquardt, A. Scarpa, and J. K. Blasie. 1977. A direct analysis of lamellar x-ray diffraction from hydrated oriented multilayers of fully functional sarcoplasmic reticulum. *Biophys. J.* 20:245–272.

Hildebrand, J. H., J. M. Prausnitz, and R. L. Scott. 1970. Regular and Related Solutions. van Nostrand Reinholdt Co., New York.

Honig, B. H., W. L. Hubbell, and R. F. Flewelling. 1986. Electrostatic interactions in membranes and proteins. *Annu. Rev. Biophys. Biophys. Chem.* 15:163–193.

Huang, C.-h., and S. Li. 1996. Computational molecular models of lipids bilayers containing mixed-chain saturated and mono-unsaturated acyl chains. *In* Handbook of Nonmedical Applications of Liposomes, Vol. 1. D. D. Lasic and Y. Barenholz, editors. CRC Press, Boca Raton, FL. 173–194.

Inoko, Y., and T. Mitsui. 1978. Structural parameters of dipalmitoyl phosphatidylcholine lamellar phases and bilayer phase transitions. *J. Phys. Soc. Jpn.* 44:1918–1924.

Israelachvili, J. N. 1985. Intermolecular and Surface Forces. Academic Press, London.

Israelachvili, J. N., and H. Wennerstrom. 1990. Hydration or steric forces between amphiphilic surfaces? *Langmuir.* 6:873–876.

Israelachvili, J. N., and H. Wennerstrom. 1992. Entropic forces between amphiphilic surfaces in liquids. *J. Phys. Chem.* 96:520–531.

Israelachvili, J. N., and H. Wennerstrom. 1996. Role of hydration and water structure in biological and colloidal interactions. *Nature.* 379: 219–225.

Janiak, M. J., D. M. Small, and G. G. Shipley. 1976. Nature of the thermal pretransition of synthetic phospholipids: dimyristoyl- and dipalmitoyllecithin. *Biochemistry.* 15:4575–4580.

Kenworthy, A. K., K. Hristova, D. Needham, and T. J. McIntosh. 1995. Range and magnitude of the steric pressure between bilayers containing phospholipids with covalently attached poly(ethyleneglycol). *Biophys. J.* 68:1921–1936.

Kim, J. T., J. Mattai, and G. G. Shipley. 1987. Gel phase polymorphism in ether-linked dihexadecylphosphatidylcholine bilayers. *Biochemistry.* 26: 6592–6598.

Klibanov, A. L., K. Maruyama, V. P. Torchilin, and L. Huang. 1990. Amphipathic polyethylene glycols effectively prolong the circulation time of liposomes. *FEBS Lett.* 268:235–237.

Kornyshev, A. A., and S. Leikin. 1989. Fluctuation theory of hydration forces: the dramatic effect of inhomogeneous boundary conditions. *Phys. Rev. A.* 40:6431–6437.

Kuhl, T. L., D. E. Leckband, D. D. Lasic, and J. N. Israelachvili. 1994. Modulation of interaction forces between bilayers exposing short-chained ethylene oxide headgroups. *Biophys. J.* 66:1479–1488.

Lasic, D. D., F. J. Martin, A. Gabizon, S. K. Huang, and D. Papahadjopoulos. 1991. Sterically stabilized liposomes: a hypothesis on the molecular origin of the extended circulation times. *Biochim. Biophys. Acta.* 1070:187–192.

Latorre, R., and J. E. Hall. 1976. Dipole potential measurements in asymmetric membranes. *Nature.* 264:361–363.

LeNeveu, D. M., R. P. Rand, V. A. Parsegian, and D. Gingell. 1977. Measurement and modification of forces between lecithin bilayers. *Biophys. J.* 18:209–230.

Lesslauer, W., J. E. Cain, and J. K. Blasie. 1972. X-ray diffraction studies of lecithin bimolecular leaflets with Incorporated fluorescent probes. *Proc. Natl. Acad. Sci. USA.* 69:1499–1503.

Lifanova, N. V., T. M. Usacheva, and V. I. Zhuravlev. 1992. The molecular structure of certain perfluorcarbons based on their equilibrium dielectric properties. *Russian J. Phys. Chem.* 66:125–126.

Lipowsky, R., and S. Grotehans. 1993. Hydration vs. protrusion forces between lipid bilayers. *Europhys. Lett.* 23:599–604.

MacDonald, R. C., and S. A. Simon. 1987. Lipid monolayer states and their relationship to bilayers. *Proc. Natl. Acad. Sci. USA.* 84:4089–4094.

Marcelja, S., and N. Radic. 1976. Repulsion of interfaces due to boundary water. *Chem. Phys. Lett.* 42:129–130.

Marra, J., and J. Israelachvili. 1985. Direct measurements of forces between phosphatidylcholine and phosphatidylethanolamine bilayers in aqueous electrolyte solutions. *Biochemistry.* 24:4608–4618.

Marrink, S.-J., M. Berkowitz, and H. J. C. Berendsen. 1993. Molecular dynamics simulation of a membrane/water interface: the ordering of water and its relation to the hydration force. *Langmuir.* 9:3122–3131.

McIntosh, T. J. 1980. Differences in hydrocarbon chain tilt between hydrated phosphatidylethanolamine and phosphatidylcholine bilayers: a molecular packing model. *Biophys. J.* 29:237–246.

McIntosh, T. J., S. Advani, R. E. Burton, D. V. Zhelev, D. Needham, and S. A. Simon. 1995. Experimental tests for protrusion and undulation pressures in phospholipid bilayers. *Biochemistry.* 34:8520–8532.

McIntosh, T. J., and P. W. Holloway. 1987. Determination of the depth of bromine atoms in bilayers formed from bromolipid probes. *Biochemistry.* 26:1783–1788.

McIntosh, T. J., A. D. Magid, and S. A. Simon. 1987. Steric repulsion between phosphatidylcholine bilayers. *Biochemistry.* 26:7325–7332.

McIntosh, T. J., A. D. Magid, and S. A. Simon. 1989a. Cholesterol modifies the short-range repulsive interactions between phosphatidylcholine membranes. *Biochemistry.* 28:17–25.

McIntosh, T. J., A. D. Magid, and S. A. Simon. 1989b. Range of the solvation pressure between lipid membranes: dependence on the packing density of solvent molecules. *Biochemistry.* 28:7904–7912.

McIntosh, T. J., R. V. McDaniel, and S. A. Simon. 1983. Induction of an interdigitated gel phase in fully hydrated lecithin bilayers. *Biochim. Biophys. Acta.* 731:109–114.

McIntosh, T. J., and S. A. Simon. 1986. The hydration force and bilayer deformation: a reevaluation. *Biochemistry.* 25:4058–4066.

McIntosh, T. J., and S. A. Simon. 1993. Contribution of hydration and steric (entropic) pressures to the interaction between phosphatidylcholine bilayers: experiments with the subgel phase. *Biochemistry.* 32: 8374–8384.

McIntosh, T. J., S. A. Simon, D. Needham, and C.-h. Huang. 1992. Interbilayer interactions between sphingomyelin and sphingomyelin: cholesterol bilayers. *Biochemistry.* 31:2020–2024.

Miller, A., C. A. Helm, and H. Mohwald. 1987. The colloidal nature of phospholipid monolayers. *J. Phys.* 48:693–701.

Mingins, J. M., D. Stigter, and K. Dill. 1992. Phospholipid interactions in model membrane systems I: experiments on monolayers. *Biophys. J.* 61:1603–1615.

Mukerjee, P., and T. Handa. 1981. Adsorption of fluorocarbon and hydrocarbon surfactants to air-water, hexane-water, and perfluorohexane-water interfaces. Relative affinities and fluorocarbon-hydrocarbon nonideality effects. *J. Phys. Chem.* 86:229802303.

Nagle, J. F., and D. A. Wilkinson. 1978. Lecithin bilayers. Density measurements and molecular interactions. *Biophys. J.* 23:159–175.

Needham, D., and E. Evans. 1988. Structure and mechanical properties of giant lipid (DMPC) vesicle bilayers from 20 degrees C below to 10 degrees C above the liquid crystal-crystalline phase transition at 24 degrees C. *Biochemistry.* 27:8261–8269.

Needham, D., T. J. McIntosh, and D. D. Lasic. 1992. Repulsive interactions and mechanical stability of polymer-grafted lipid membranes. *Biochim. Biophys. Acta.* 1108:40–48.

Ninham, B. W., and V. A. Parsegian. 1970. Van der Waals forces. *Biophys. J.* 10:646–663.

O'Brien, F. E. M. 1948. The control of humidity by saturated salt solutions. *J. Sci. Instrum.* 25:73–76.

Papahadjopoulos, D., T. M. Allen, A. Gabizon, E. Mayhew, K. Matthay, S. K. Huang, K.-D. Lee, M. C. Woodle, D. D. Lasic, C. Redemann, and F. J. Martin. 1991. Sterically stabilized liposomes: improvements in pharmacokinetics and antitumor therapeutic efficacy. *Proc. Natl. Acad. Sci. USA.* 88:11460–11464.

Parsegian, V. A., N. Fuller, and R. P. Rand. 1979. Measured work of deformation and repulsion of lecithin bilayers. *Proc. Natl. Acad. Sci. USA.* 76:2750–2754.

Parsegian, V. A., and B. W. Ninham. 1969. Application of the Lifshitz theory to the calculation of van der Waals forces across thin lipid films. *Nature.* 224:1197–1198.

Pearson, R. H., and I. Pascher. 1979. The molecular structure of lecithin dihydrate. *Nature.* 281:499–501.

Privitera, N., R. Naon, P. Vierling, and J. G. Riess. 1995. Phagocytic uptake by mouse peritoneal macrophages of microspheres coated with phosphocholine or polyethylene glycol phosphate-derived perfluoroalkylated surfactants. *Int. J. Pharm. (Amst.).* 120:73–82.

Rand, R. P., and V. A. Parsegian. 1989. Hydration forces between phospholipid bilayers. *Biochim. Biophys. Acta.* 988:351–376.

Ravily, V., S. Gaentzler, C. Santaella, and P. Vierling. 1996. Synthesis of highly fluorinated ether glycerophospholipids and evaluation of their biological tolerance. *Helv. Chim. Acta.* 79:405–425.

Reyes, J. F. Greco, R. Motais, and R. Latorre. 1983. Phloretin and phloretin analogues: mode of action. *J. Memb. Biol.* 72:93–103.

Riess, J. G. 1994. highly fluorinated systems for oxygen transport, diagnosis and drug delivery. *Colloids Surf. A. Physicochem. Eng. Aspects.* 84:33–48.

Riess, J. G., F. Frézard, J. Greiner, M.-P. Krafft, C. Santaella, P. Vierling, and L. Zarif. 1996. Membranes, vesicles and other supramolecular systems made from fluorinated amphiphiles. *In* Handbook of Non-Medical Applications of Liposomes, Vol. 3. Y. Barenholz and D. D. Lasic, editors. CRC Press, Boca Raton, FL. 97–141.

Rolland, J.-P., C. Santaella, and P. Vierling. 1996. Molecular packing of highly fluorinated phosphatidylcholines in monolayers. *Chem. Phys. Lipids.* 79:71–77.

Ruocco, M. J., D. J. Siminovitch, and R. G. Griffin. 1985. Comparative study of the gel phase of ether- and ester-linked phosphatidylcholines. *Biochemistry.* 24:2406–2411.

Santaella, C., F. Frézard, P. Vierling, and J. G. Riess. 1993. Extended in vivo blood circulation time of fluorinated liposomes. *FEBS Lett.* 336: 481–483.

Santaella, C., and P. Vierling. 1995. Molecular order and mobility within liposomal membrane made from highly fluorinated phospholipids. *Chem. Phys. Lipids.* 77:173–177.

Santaella, C., P. Vierling, and J. G. Riess. 1991. New perfluoroalkylated phospholipids as injectable amphiphiles. Synthesis, preliminary physicochemical and biocompatibility data. *New J. Chem.* 15:685–692.

Santaella, C., P. Vierling, and J. G. Riess. 1992. Perfluoroalkylated phospholipids as surfactants and co-surfactants for injectable emulsions. *Biomater. Artif. Cells Immobilization Biotechnol.* 20:835–837.

Santaella, C., P. Vierling, J. G. Riess, T. Gulik-Krzywicki, A. Gulik, and B. Monasse. 1994. Polymorphic phase behavior of perfluoroalkylated phosphatidylcholines. *Biochim. Biophys. Acta.* 1190:25–39.

Semple, S. C., A. Chonn, and P. R. Cullis. 1996. Influence of cholesterol on the association of plasma proteins with liposomes. *Biochemistry.* 35:2521–2525.

Serrallach, E. N., R. Dijkman, G. H. de Haas, and G. G. Shipley. 1983. Structure and thermotropic properties of 1,3-dipalmitoyl-glycero-2-phosphocholine. *J. Mol. Biol.* 170:155–174.

Shannon, C. E. 1949. Communication in the presence of noise. *Proc. Inst. Radio Eng. N.Y.* 37:10–21.

Simon, S. A., S. Advani, and T. J. McIntosh. 1995. Temperature dependence of the repulsive pressure between phosphatidylcholine bilayers. *Biophys. J.* 69:1473–1483.

Simon, S. A., C. A. Fink, A. K. Kenworthy, and T. J. McIntosh. 1991. The hydration pressure between lipid bilayers: a comparison of measurements using x-ray diffraction and calorimetry. *Biophys. J.* 59:538–546.

Simon, S. A., and T. J. McIntosh. 1986. The depth of water penetration into lipid bilayers. *Methods Enzymol.* 127:511–521.

Simon, S. A., and T. J. McIntosh. 1989. Magnitude of the solvation pressure depends on dipole potential. *Proc. Natl. Acad. Sci. USA.* 86: 9263–9267.

Simon, S. A., and T. J. McIntosh. 1991. Surface ripples cause the large fluid spaces between gel phase bilayers containing cholesterol. *Biochim. Biophys. Acta.* 1064:69–74.

Simon, S. A., T. J. McIntosh, A. D. Magid, and D. Needham. 1992. Modulation of the interbilayer hydration pressure by the addition of dipoles at the hydrocarbon/water interface. *Biophys. J.* 61:786–799.

Smaby, J. M., and H. L. Brockman. 1990. Surface dipole moments of lipids at the argon-water interface. Similarities among glycerol-ester-based lipids. *Biophys. J.* 58:195–204.

Smaby, J. M., H. L. Brockman, and R. E. Brown. 1994. Cholesterol's interfacial interactions with sphingomyelins and phospatidylcholines: hydrocarbon chain structure determines the magnitude of condensation. *Biochemistry.* 33:9135–9142.

Smejtek, P. 1995. Permeability of lipophilic ions across lipid bilayers. *In* Permeability and Stability of Lipid Bilayers. E. A. Disalvo and S. A. Simon, editors. CRC Press, Boca Raton, FL. 197–240.

Sturtevant, J. M., C. Ho, and A. Reiman. 1979. Thermotropic behavior of some fluoro dimyristoylphosphatidylcholines. *Proc. Natl. Acad. Sci. USA.* 76:2239–2243.

Tardieu, A., V. Luzzati, and F. C. Reman. 1973. Structure and polymorphism of the hydrocarbon chains of lipids: a study of lecithin-water phases. *J. Mol. Biol.* 75:711–733.

Taylor, D. M., O. N. Oliveira, and H. Morgan. 1990. Models for interpreting surface potential measurements and their application to phospholipid monolayers. *J. Colloid Interface Sci.* 139:508–518.

Tiddy, C. G. T. 1985. Concentrated surfactants systems. *In* Modern Trends of Colloid Science in Chemistry and Biology. E. Eicke, editor. Birkaüser Verlag, Basel. 148.

Torbet, J., and M. H. F. Wilkins. 1976. X-ray diffraction studies of lecithin bilayers. *J. Mol. Biol.* 62:447–458.

Tristram-Nagle, S., and S. R. Dowd. 1994. X-ray diffraction study of three $^{19}$F-labeled dimyristoylphosphatidylcholines. *J. Phys. Chem.* 98: 4469–4472.

Tristram-Nagle, S., R. Zhang, R. M. Suter, W. C. R., W.-J. Sun, and J. F. Nagle. 1993. Measurement of chain tilt angle in fully hydrated bilayers of gel phase lecithins. *Biophys. J.* 64:1097–1109.

Vierling, P., C. Santaella, and J. G. Riess. 1995. Fluorinated liposomes. *In* Liposomes: New Systems and New Trends in Their Applications. F. Puisieux, P. Couvreur, J. Delattre, and J. P. Devissaguet, editors. Edition de Santé, Paris. 293–318.

Vogel, V., and D. Möbius. 1988. Local surface potentials and electric dipole moments of lipid monolayers: contributions of the water/lipid and the lipid/air interfaces. *J. Colloid Interface Sci.* 126:408–420.

Wolf, S. G., M. Deutsch, E. M. Landau, M. Lahav, L. Leiserowitz, K. Kjaer, and J. Als-Nielsen. 1988. A synchrotron x-ray study of a solid-solid phase transition in a two-dimensional crystal. *Science.* 242: 1286–1290.

Woodle, M. C., L. R. Collins, E. Sponsler, N. Kossovsky, D. Papahadjopoulos, and F. J. Martin. 1992. Sterically stabilized liposomes. Reduction in electrophoretic mobility but not electrostatic surface potential. *Biophys. J.* 61:902–910.

Worcester, D. L., and N. P. Franks. 1976. Structural analysis of hydrated egg lecithin and cholesterol bilayers. II. Neutron diffraction. *J. Mol. Biol.* 100:359–378.

Zheng, C., and G. Vanderkooi. 1992. Molecular origin of the internal dipole potential in lipid bilayers: calculation of the electrostatic potential. *Biophys. J.* 63:935–941.

Zhou, F., and K. Schulten. 1995. Molecular dynamics study of a membrane-water interface. *J. Phys. Chem.* 99:2194–2207.